THE OPTICAL MODEL OF THE NUCLEUS IN THE LIGHT OF PRESENT-DAY DATA

I. S. SHAPIRO

Usp. Fiz. Nauk 75, 61-100 (September, 1961)

INTRODUCTION

THE development of nuclear physics in the course of the past few years has led to many unexpected results which essentially change our picture of the structure of the nucleus and the dynamics of nuclear processes. Briefly speaking, we have seen the tremendous importance of collective effects which give rise to the appearance of qualitatively new phenomena.

The subject of the present survey is the so-called optical model of the nucleus, a model according to which nucleons are scattered by nuclei in almost the same way as light is scattered by a semi-transparent optical medium. The important thing here is just this semi-transparency of the nucleus since, on the basis of the data concerning effective cross sections for the interaction of free nucleons, one would have expected the nucleus to behave like a black body in scattering processes.

The optical model for the scattering of nucleons has been investigated by comparing the theoretical and experimental data, beginning approximately with the years 1953 — 1954, after the appearance of the papers of Feshbach, Porter, and Weisskopf.[1,2] Although certain important details, concerning which we shall have to speak later on, still remain unclear, one can hardly doubt now that the optical model of the nucleus correctly describes nucleon scattering.

In 1958 — 1960 there was published a series of experimental and theoretical investigations whose results appeared at first glance to be completely fantastic. We have in mind the experiments on elastic scattering by nuclei of complex particles—deuterons, α particles, N^{14}, O^{16}, and other nuclei. As a result of the progress of experimental technique, one succeeded in these experiments in obtaining detailed pictures of the angular distributions of the scattered particles and, in particular, the differential cross sections for scattering through large angles. A comparison of the results obtained with the theory showed that the scattering of these complex particles is well described by the optical model and, in fact, with approximately the same parameters as for nucleons. In other words, it appears that the nucleus is almost equally transparent for complex particles as it is for nucleons. This remarkable fact, if it should be confirmed by further investigations, has great importance for an understanding of the dynamics of nuclear reactions and, in particular, of reactions of the so-called direct type, which proceed without the preliminary stage of formation of a compound nucleus. The results described concerning the scattering of composite particles will be treated in more detail in the second part of this survey. The first part is devoted to a description of the present state of the optical model for nucleons.

I. THE OPTICAL MODEL FOR SCATTERING OF NUCLEONS

1. Initial Assumptions

The optical model attempts to obtain the following quantities: the cross section for elastic scattering σ_S, the total cross section for all inelastic processes (the so-called reaction cross section) σ_r, the differential scattering cross section at a given angle ϑ: $d\sigma_S(\vartheta)$ and the polarization of the scattered nucleons $P(\vartheta)$ as a function of the scattering angle ϑ.

The fundamental assertion which constitutes the essence of the model consists in the statement that the scattering of nucleons by complex nuclei can be described as a solution of the problem of diffraction of the nucleon wave by a certain potential. This means that the scattering problem is treated not as a many-body problem, but as a problem of motion of a nucleon in a certain time-independent field produced by the nucleus. Thus the Schrödinger equation for the nucleon wave function $\Psi(\mathbf{r})$ has the form:

$$\left(\nabla^2 + k^2 - \frac{2m}{\hbar^2} U(\mathbf{r})\right)\Psi(\mathbf{r}) = 0, \tag{1}$$

where

$$k = \frac{\sqrt{2mE}}{\hbar} \tag{2}$$

is the wave number of the nucleon, and $U(\mathbf{r})$ is the nuclear potential. We seek a solution of Eq. (1) which at large distances from the nucleus has the form of a superposition of an incident plane wave with wave vector $\mathbf{k}$ and a diverging spherical wave:

$$\Psi(\mathbf{r}) = e^{i\mathbf{kr}} + f(\mathbf{k},\mathbf{k}')\frac{e^{ikr}}{r}, \tag{1a}$$

where $\mathbf{k}$ is the wave vector of the scattered particle ($|\mathbf{k}'| = |\mathbf{k}|$). The amplitude of the outgoing wave $f(\mathbf{k}, \mathbf{k}')$ depends on $\mathbf{k}$ and the scattering angle ϑ. The complex quantity f has the dimensions of a length and is called the scattering amplitude. The square modulus of the scattering amplitude determines the differential scattering cross section:

$$d\sigma_s(\vartheta) = |f(\mathbf{k},\mathbf{k}')|^2 d\Omega, \tag{1b}$$

where $d\Omega = \sin\vartheta\, d\vartheta\, d\varphi$ is the element of solid angle. The scattering cross section σ_s is equal to the integral of (1b) over all scattering angles ϑ:

$$\sigma_s = 2\pi \int_0^\pi |f|^2 \sin\vartheta\, d\vartheta. \tag{1c}$$

The total cross section $\sigma_t = \sigma_r + \sigma_s$ is expressed in terms of the imaginary part of the forward scattering amplitude (i.e., the amplitude at $\vartheta = 0$):

$$\sigma_t = \frac{4\pi}{k} \operatorname{Im} f(\vartheta = 0). \tag{1d}$$

Finally, the absorption cross section σ_r is given by the formula

$$\sigma_r = \sigma_t - \sigma_s = \frac{4\pi}{k} \operatorname{Im} f(\vartheta = 0) - 2\pi \int_0^\pi |f|^2 \sin\vartheta\, d\vartheta. \tag{1e}$$

The parameters determining the potential $U(\mathbf{r})$ (its depth, extension, etc.) are found by comparing the experimental cross sections with those calculated using formula (1). Of course, the model has a meaning only if the parameters of the potential are either the same over the whole range of energy of the incident nucleons and for all nuclei, or (which is actually the case) vary only slightly. Since, in addition to scattering, there occurs an absorption of the particles, it is clear that the potential $U(\mathbf{r})$ must be complex. This follows from the fact that the current density of the particles is given by the usual expression

$$\mathbf{j}(\mathbf{r}) = -\frac{i\hbar}{2m}(\Psi^* \nabla\Psi - \Psi \nabla\Psi^*), \tag{3}$$

and it then follows immediately from (1) that

$$\operatorname{div} \mathbf{j} = 2 \operatorname{Im} U\, |\Psi|^2. \tag{4}$$

If the nucleus absorbs particles, div $\mathbf{j}$ at points of the nucleus must be different from zero and negative. Consequently

$$-\operatorname{Im} U \equiv W > 0. \tag{5}$$

The sign of the real part of the potential is chosen so that it corresponds to an attractive force between the nucleon and the nucleus:

$$-\operatorname{Re} U \equiv V > 0. \tag{6}$$

Thus

$$U(\mathbf{r}) = -V(\mathbf{r}) - iW(\mathbf{r}). \tag{7}$$

It is important to emphasize that the imaginary part of the potential is important not only for the calculation of the reaction cross section σ_r (which is different from zero only for $W \neq 0$), but also for the calculation of the scattering cross sections $d\sigma_s(\vartheta)$ and σ_s.

The point is that, from the very fact of the occurrence of absorption of incident nucleons by the nucleus, independent of whatever mechanism one uses for this absorption there results a definite scattering of nucleons. This occurs because, in nuclear physics, scattering always occurs even under the conditions $\lambda \ll R$ (where R is the nuclear radius, and λ is the de Broglie wavelength of the nucleon) as a diffraction problem. In this sense the situation is markedly different from ordinary optics—the scattering of light by optically inhomogeneous media. (In the case of scattering of light, for wavelengths which are much smaller than the dimensions of the inhomogeneities of the medium, it becomes valid to use the laws of geometrical optics, and diffraction phenomena play no role.)

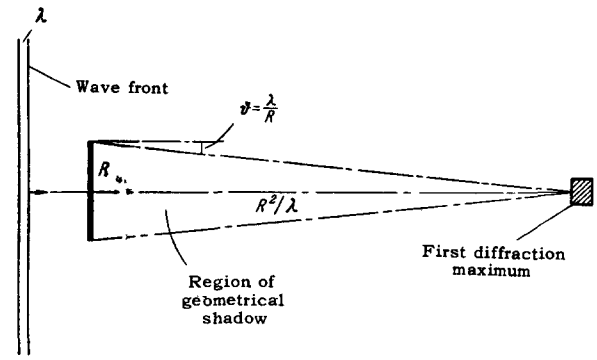

FIG. 1. Diffraction by a black disc.

In order to explain the situation, let us consider Fraunhofer diffraction of waves by a black disc of radius R under the condition that $\lambda \ll R$. We know that in this case, beyond the disc at some distance from it there appears a bright spot—the first diffraction maximum. In the language of geometrical optics this means that part of the light rays were scattered, and the directions of the scattered rays make an angle $\vartheta \gtrsim \lambda/R$ with the initial ray (Fig. 1). However, since the diffraction angle ϑ is small, there will still be a region of geometrical shadow near the disc. "Near" in this case means a distance which is small compared to the distance from the bright spot. This distance is equal to $R/\vartheta = R^2/\lambda$. Thus a diffraction picture appears only starting with a distance of the order of R^2/λ. In other words, if we make an observation at distances of the order of or greater than R^2/λ, we "see" diffracted rays, i.e., we observe scattering resulting from diffraction. But at distances smaller than R^2/λ, we observe a picture corresponding to geometrical optics. In optics $\lambda \cong 10^{-5}$ cm, $R \simeq 1$ cm and, consequently, $R^2/\lambda \simeq 1$ km, while the observations occur at distances which are much smaller than this quantity, i.e., in regions where the wave field is described to high accuracy by the geometric approximation. In nuclear physics $R \simeq 10^{-12}$ cm, $\lambda \gtrsim 10^{-13} - 10^{-14}$ cm, and $R^2/\lambda \lesssim 10^{-11} - 10^{-10}$ cm, whereas the observation of the scattering occurs at macroscopic distances, which are much greater than this quantity, i.e., just where the distortion of the wave field as a result of diffraction essentially determines the whole picture. It is not difficult to compute the effective scattering cross section, i.e., the ratio of the intensity of the diffracted waves to the flux density in the incident

wave. For this purpose we use the Babinet reciprocity law, according to which the diffraction picture behind the black disc coincides exactly with the diffraction picture behind a hole of the same radius in a black screen, if, in this latter case, we replace all the maxima by minima, (i.e., just as a negative and positive of the same photograph coincide with one another). Since at a distance of R^2/λ beyond the hole there will be a black spot, in the same way, in terms of scattering, this means that all the light passing through the aperture (or, consequently, impinging on the black disc) undergoes scattering.

From this it is clear that the intensity of the scattered light is equal to $J\pi R^2$, where J is the current density in the incident waves. Thus, for the cross section for scattering by a black disc, we have

$$\sigma_s = \frac{J\pi R^2}{J} = \pi R^2. \tag{8}$$

With regard to the scattering of nucleons by nuclei, the result we have obtained means that if the nucleus is "black," i.e., if every nucleon incident upon it does not leave (or emerges leaving some of its energy in the nucleus), then the total cross section $\sigma_t = \sigma_s + \sigma_r$ for interaction of the nucleon with the nucleus will be equal to $2\pi R^2$, since obviously

$$\sigma_r = \pi R^2. \tag{9}$$

This result, which follows automatically from the wave picture, seems paradoxical if we do not consider the wave nature of the scattering, and go over to particle language. In the derivation of formula (8) we have assumed that the disc is black, i.e., we have assumed that there is no reflection of the wave at the surface of the disc. (In the contrary case we could not apply the Babinet principle.) Such an assumption corresponds to equating the real part of the potential to zero. All the scattering in this case results solely from the fact that there is a total absorption of the particles impinging on the nucleus.

In closing the consideration of what we might call the general physical aspect of the theory of scattering of nucleons by nuclei, we emphasize once more that any, even local, disturbance of a wave field leads, as a result of continuity and the continuity of the first derivatives of the wave function, to a change in the field at far distances, i.e., in particular, to scattering. Just because of this circumstance, the scattering of nucleons by nuclei is inseparably coupled to the absorption, and this means that it is coupled to the imaginary part of the optical potential, if the scattering is described by an optical model.

From these remarks, besides, it follows that if the nucleus were assumed to be "black" for the incident nucleons, then in calculating the values of the scattering and reaction cross sections we would need no additional models. It is obvious that the nucleus can be considered to be "black" if the average mean free path of a nucleon impinging on the nucleus is much less than nuclear dimensions. An estimate of this quantity can be obtained using the formula

$$\Lambda = \frac{1}{\rho\sigma}, \tag{10}$$

where σ is the collision cross section for the incident nucleon with the nucleons in the nucleus, ρ is the density of particles in the nucleus. The value of ρ is a constant to good accuracy for all nuclei:

$$\rho \simeq 10^{38}\,\mathrm{cm}^{-3}.$$

If we choose for σ the value of the cross section for collision of free nucleons with a kinetic energy in the center of mass system of the order of several tens of Mev, then $\sigma \simeq 0.5$ barn and

$$\Lambda = 2\cdot 10^{-14}\ \mathrm{cm}, \tag{10a}$$

which is much less than the radius of even the light nuclei, for which $R \simeq 4 - 5 \times 10^{-13}$ cm. With such a mean free path, the probability that the nucleon passes through the nucleus without suffering a collision is very small (approximately 10^{-8}). Starting from just such estimates, it was assumed for a long time that the nucleus is a black body, and that therefore for nucleon energies of the order of 10 Mev, where the condition $\lambda \ll R$ is fulfilled, σ_s and σ_r should be determined by (9) and (10). These formulas predict a monotonic increase of cross section with increasing mass number, since

$$R = r_0 A^{1/3}, \tag{11}$$

and constancy of the cross section as a function of energy, if the latter is such that $\lambda \ll R$.

The model of a black nucleus also predicts a monotonic increase in cross section with increasing A and fall off with increasing E for low energies of nucleons in all those cases where no resonance effects can occur resulting from isolated levels of the compound nucleus.

Experiments did not confirm these expectations. It first became clear from the data of Barschall et al[3] that for neutrons with energies up to 3 Mev the cross sections σ_s and σ_r as a function of A and the energy of the incident neutrons E are not monotonic, but show a behavior which is incompatible with the picture of a black nucleus. Further experimental investigations of angular distributions of scattered neutrons and protons also were in poor agreement with the idea of a black nucleus. At the same time, it appeared that all of these data are very satisfactorily described by the optical model. The parameters of the optical model are discussed in detail in Sec. 2; here we shall only say in a preliminary fashion that the magnitude of the imaginary part of the potential W for nucleon energies of the order of 10 Mev is around 5 — 6 Mev. Let us see what mean free path of the nucleon in the nucleus corresponds to this value.

For simplicity we shall assume that $V(\mathbf{r})$ and $W(\mathbf{r})$ are constant inside the nucleus and that the nucleus is infinite in size. (This can be assumed for estimates, since $\lambda \ll R$.) Under these simplifying assumptions the nucleus can be pictured as a half-plane and the flux of nucleons occurs normal to its boundary.

Then it follows from the Schrödinger equation that inside the nucleus the wave function of the nucleon has the form of a plane wave

$$\Psi(\mathbf{r}) = Ce^{i\mathbf{K}\mathbf{r}}, \tag{12}$$

where

$$K = \frac{1}{\hbar}\sqrt{2m(E+V+iW)} \tag{13}$$

and C is a coefficient determined from the requirement of continuity of the wave function and its derivatives at the nuclear boundary. Equation (13) shows that because the potential is complex, the wave vector of the nucleon inside the nucleus also is a complex quantity. If we assume that $W \ll V$ (which actually corresponds to the true situation, since $W \simeq 5-6$ Mev, while $V \simeq 40-50$ Mev), then

$$\operatorname{Re} K \equiv K_1 = k\sqrt{1+\frac{V}{E}},$$

$$\operatorname{Im} K \equiv K_2 = \frac{1}{2}k\frac{W}{E}\cdot\frac{1}{\sqrt{1+V/E}}. \tag{14}$$

From (14) we see, besides, that the real part of the potential determines the real part of the "index of refraction" of the nucleus, if we use optical terminology. In fact, in optics the index of refraction of a medium is equal to the ratio of the wavelength in vacuum to the wavelength in the medium, or to the reciprocal of the ratio of the wave numbers. If, in this same way, we introduce a nuclear index of refraction n, then

$$n_1 \equiv \operatorname{Re} n = \frac{K_1}{k} = \sqrt{1+\frac{V}{E}}\,,\quad n_2 = \operatorname{Im} n = \frac{K_2}{k} = \frac{1}{2}\frac{W}{E}\frac{1}{\sqrt{1+V/E}}.$$

Thus, the greater the real part of the potential, the stronger the refraction and reflection of the nucleon wave at the nuclear boundary. Precisely as in optics, the imaginary part of the index of refraction determines the damping of the wave in the medium as a result of absorption. From formulas (12) and (14) it follows that the wave function $\Psi(\mathbf{r})$ contains a damping factor ($\mathbf{K}_2\cdot\mathbf{r} > 0$)

$$\Psi(\mathbf{r}) = Ce^{-\mathbf{K}_2\mathbf{r}}e^{i\mathbf{K}_1\mathbf{r}}. \tag{15}$$

For neutrons with an energy of 14 Mev, $1/k = \lambda\!\!\!^{-} = 1.4 \times 10^{-13}$ cm, $W \simeq 5$ Mev, $V \simeq 40$ Mev. We then obtain from formula (15)

$$2\Lambda = \frac{1}{K_2} = 2\frac{E}{W}\lambda\!\!\!^{-}\sqrt{1+\frac{V}{E}} = 1{,}2\cdot 10^{-12}\ \text{cm}, \tag{16}$$

i.e., a quantity which is 30 times greater than that calculated by us earlier from formula (10), in which we used for the collision cross section σ of the incident nucleon with the nucleons in the nucleus the experimental value of σ for the collisions of free nucleons. From a comparison of these data we see that the effective cross section for collision with a nucleon bound in the nucleus is 30 times smaller than the cross section for free nucleons.

The main reason for the reduction in cross section for bound nucleons is the action of the Pauli principle. In order to explain this, let us assume, in accordance with the shell model, that the nucleons in a nucleus move independently of one another. In the model of an infinite nucleus this means that the nucleons in the nucleus in their ground state form a gas of Fermi particles, in which all the lowest energy states are occupied (degenerate Fermi gas). The momentum distribution of the nucleons in such a gas is characterized by the fact that there is a certain limiting momentum (the radius of the Fermi sphere), while all states with momenta less than the radius of the Fermi sphere are occupied, since the nucleus is in its ground (i.e., lowest) energy state. If an external nucleon impinges on the nucleus, then we can say that a collision has occurred between it and the nucleons inside the nucleus only when the momenta of the colliding particles, including also the momentum of the nucleon inside the nucleus, have changed. In the case of a collision of free nucleons, we may have any change in momenta of the colliding particles (which is compatible with the conservation laws). But the momentum of a nucleon inside the nucleus can change only in such a way that the final state in which the nucleon is put as a result of the collision is not occupied, i.e., is located outside the Fermi sphere. This means that, for nucleons having momenta considerably less than the radius of the Fermi sphere, collisions with small transfer of momentum are impossible (only for the very small number of nucleons which are contained in the boundary layer of the Fermi distribution can one have arbitrarily small momentum transfers, so that collision with these particles occurs almost in the same way as with free nucleons). The restriction in the number of possible final states as a result of this effect leads to a reduction of the cross section by reducing the available phase volume.

In these arguments the nucleus was assumed to be infinite in extent. However, nothing is changed if we take account of the finite dimensions of the nucleus. The only difference will be that the state of the nucleons inside the nucleus is characterized in this case not by a definite value of the momentum, but by the values of the energy and angular momentum. The role of the radius of the Fermi sphere is then taken over by the energy of the highest occupied state, and in place of the restricted possibilities for momentum transfer to the nucleon in the infinite nucleus because of the Pauli principle, we must now speak of the possibilities of transition of a nucleon in these collisions only to states which lie above the highest occupied energy level.

Of course, it is understood that the action of the Pauli principle should lead to a reduction of the cross section for collision with bound nucleons inside the nucleus as compared with the cross section for free nucleons, since this is qualitatively clear even before one establishes the values of the parameters of the optical model. However, the magnitude of this reduction in cross section (and consequently the increase in transparency of the nucleus) was only explained after comparing computations on the optical model with the experimental data, and turned out to be unexpectedly large.

2. Parameters of the Optical Potential

a) The simplest potential—the rectangular well. This potential was used for scattering of neutrons in the first papers of Feshbach, Porter, and Weisskopf.[1,2] The imaginary part of the potential was also taken to be constant inside the nucleus and equal to zero outside it. Thus

$$U(\mathbf{r}) = -V(\mathbf{r})(1 + i\zeta), \tag{17}$$

where

$$V(r) = \begin{cases} V_0, & r < R, \\ 0, & r > R, \end{cases} \qquad \zeta = \frac{W}{V_0}. \tag{18}$$

For neutrons with energies up to 3 Mev, the best agreement of the theoretical computations with the experimental data for the total cross section σ_t was obtained for the following choice of parameters:

$$V_0 = 42 \text{ Mev}, \ \zeta = 0.03, \quad R = 1{,}45 \cdot 10^{-13} A^{1/3} \text{ cm}. \tag{19}$$

We shall not give a detailed analysis of the results of computations with the potential (17) as compared with the experimental data, since at present the defects of the potential (17) are well understood. The main defects are that a model with a rectangular well gives too high values of the ratio $\sigma_0 = \sigma_s/\sigma_r$. This is the case even when the energy of the incident neutrons is so small that the wavelength of the neutron is $\lambda \gg R$. At first glance, such a situation seems strange since the nuclear forces fall off quite rapidly with distance, and a "smearing" of the potential should occur over a distance of the order of 10^{-13} cm, which is much less than the wavelength of the incident neutron, if its energy is of the order of 200 kev or less. Under these conditions it would appear that the nature of the fall-off of the potential (infinitely rapid or with a derivative of the order of 4×10^{15} Mev cm^{-1}) should not essentially affect the results. In these considerations, however, one has disregarded the fact that, however small the energy of the nucleon outside the nucleus, inside the nucleus its wavelength cannot be greater than $\lambda\!\!\!^{-}_1 = \hbar/\sqrt{2mV_0}$. For $V_0 \simeq 40$ Mev, $\lambda\!\!\!^{-}_1 = 0.7 \times 10^{-13}$ cm, and this is already comparable with the distance over which the potential should fall off significantly. The sharp jump in wave number at the nuclear boundary makes more difficult the penetration of neutrons into the nucleus, since most of the neutron wave undergoes reflection. In this respect the present situation is entirely analogous to the optical case: a jump in the index of refraction at the boundary between two media leads to the appearance of reflected waves whose intensity is the greater, the greater the discontinuity in the index of refraction.

Just as the elimination of jumps in the index of refraction increases the light output of an optical apparatus (so-called translucent optics), a smooth fall-off to zero in the potential U(r) should lead to an increase in the cross section σ_r, a reduction of σ_s, and, consequently, an approach of the theoretical value of σ_0 to the experimental data. This is why the next step in the development of the optical model was the treatment of the nucleus with a "smeared boundary," i.e., a potential which falls off continuously to zero.

b) Nucleus with diffuse edge. The optical model with a smooth fall-off in the nuclear potential was first treated by Woods and Saxon[4] (for protons) and by Nemirovskii[5] for neutrons. Later on, the nucleus with a diffuse edge was treated by many authors, and from these papers it appeared that the shape of the curve of fall-off of the potential does not play any essential role so long as one guarantees a sufficiently rapid fall-off. Most frequently one uses the Woods-Saxon potential

$$V(r) = V_0 f(r), \qquad f(r) = \frac{1}{1 + e^{(r-R)/a}}. \tag{20}$$

The rate of fall-off of the potential is characterized by the parameter a. As follows from numerous experimental data,

$$a = 0{,}65 \cdot 10^{-13} \text{ cm}. \tag{20a}$$

For the "nuclear radius" R, the best value, when one uses the Woods-Saxon potential, is

$$R = 1.27 \cdot 10^{-13} \text{ cm } A^{1/3}. \tag{21}$$

This value is somewhat lower than that used by Feshbach, Porter, and Weisskopf,[2] which is natural since the potential (20) is different from zero also for r > R. In the paper of Luk'yanov, Orlov, and Turovtsev,[6] they used a potential which coincides with a cubic parabola (Fig. 2):

$$V(r) = V_0 f(r), \tag{22}$$

$$f(r) = \begin{cases} 1, & r \leqslant R - d, \\ 1 + \frac{(r-R-2d)(r-R+d)^2}{4d^3}, & R - d \leqslant r \leqslant R + d, \\ 0, & r \geqslant R + d. \end{cases} \tag{22a}$$

The rate of fall-off of the potential is here determined by the quantity d. The best value of d is

$$d = 3{,}66 \cdot 10^{-13} \text{ cm}. \tag{23}$$

The parameter R in formula (22a) was chosen by the authors of reference 6 in the form

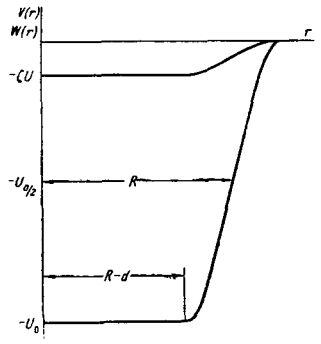

FIG. 2. Nuclear potential used for calculating $d\sigma_s$, σ_s, and σ_r for 14-Mev neutrons in reference 6.

$$R=(1.27A^{1/3}+0,3)\cdot 10^{-13}\ \text{cm}. \qquad (24)$$

It should be mentioned that from data on scattering and capture cross sections it is not possible to determine V_0 and R uniquely. Actually, other things being equal, all the results depend on V_0R^2. The potential (22), although less "physical," is convenient for computation since the fall-off of V(r) to zero for $r \geq R + d$ (in place of the exponential damping of the Wood-Saxon potential) greatly reduces the computation time for a digital computer, without which it would be impossible to attempt a solution of the Schrödinger equation (1) for the case of a nucleus with a diffuse boundary. It is absolutely necessary that the imaginary part of the potential W(r) depend on r in the same way as the real part. However, in the first papers on the model with a diffuse edge, the authors attempted to use the minimal number of parameters, and so they chose for the imaginary part of the potential the same dependence as for the real part. In other words, they assumed that

$$U(r)=-V(r)(1+i\zeta). \qquad (25)$$

The value of the quantities V_0 and ζ depends on the energy of the nucleon. Thus, for neutrons with energy 14 Mev the best agreement with the experimental data for the potential (22) is obtained for the values

$$V_0=42, \quad \zeta=0,12, \qquad (26)$$

which corresponds to W = 5.05 Mev. Approximately

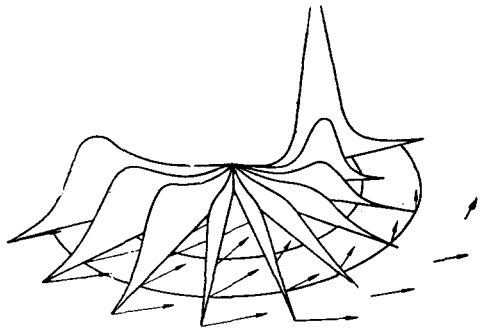

FIG. 3. Value of | div j | for 18-Mev α particles at various points in an argon nucleus. The interior circle corresponds to a value of the nuclear potential equal to 0.9 V_0, the outer circle to 0.1 V_0. The arrows indicate the direction of j.

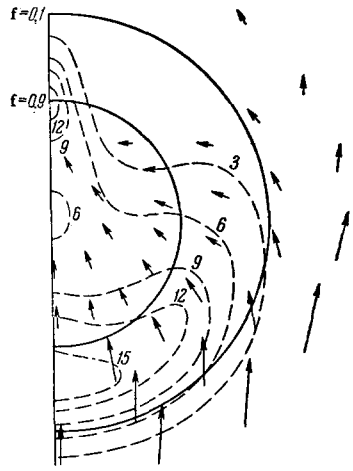

FIG. 4. The three-dimensional picture of Fig. 3 as projected on a plane. The arrows show the magnitude and direction of j. The level lines (dashed lines) are drawn through points with the same values of | div j |.

the same values for these quantities are obtained at E = 14 Mev for the Woods-Saxon potential. The parameters R and D [or a in the potential (20)], V_0, and ζ were selected to give the best agreement between computational and experimental values of σ_s and σ_r. Using the parameters thus obtained, the differential scattering cross section $d\sigma_s(\vartheta)$ was calculated, which could also be compared with the results of experiments and thus test the model. In the variant considered by us, the imaginary part of the potential W is different from zero at all points of the nucleus. It takes on its maximum value in the central region of the nucleus and falls off with increasing radius (cf. Fig. 2). However, this does not mean that absorption of the nucleons occurs mostly in the center rather than at the periphery of the nucleus. The point is that, as we have already said, the absorption of particles at a given point in the nucleus is determined by the magnitude of the divergence, which is proportional not just to W(r), but also to the density of incident particles $|\Psi(\mathbf{r})|^2$ at the given point r in the nucleus. Figure 3 shows the effect of the factor $|\Psi(\mathbf{r})|^2$ in the expression for the divergence. In this figure, we show some computations of McCarthy[7] made on the basis of the optical model with volume absorption, for α particles of 18 Mev energy impinging on argon nuclei. The heights of the points in the diagram of Fig. 3 give the value of − div j; the magnitudes and directions of the arrows approximately show the current j. The computations were done for the Woods-Saxon potential, where the two circles in Fig. 3 correspond to distances at which the potential is equal to 0.9 V_0 and 0.1 V_0 respectively.

As we see from Fig. 3, the absorption is not uniformly distributed over the nucleus, even though W(r) changes very little in the central part. A point of interest also is the presence of a large maximum in the absorption in the direction of the incident beam, at the edge of the nucleus diametrically opposite to the side from which the impinging particles came. Approximately 15 — 20% of all the particles absorbed by the nucleus are absorbed in this maximum. Figure 4 shows the same picture in a plane view. The dashed

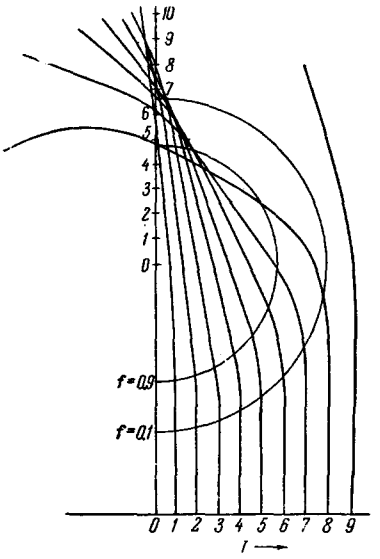

FIG. 5. Explanation of the appearance of a maximum in |div j| at the edge of the nucleus. In the figure is shown the geometric path of "rays" (normals to wave surfaces) for 30-Mev neutrons in an argon nucleus. Because of the refraction effect of the real part of the nuclear potential, the nucleus acts as a lens with a focus at the edge of the nucleus. The distances from the center of the nucleus are given in units of 10^{-13} cm (fermi).

lines are lines of "equal height," i.e., lines along which the divergence is constant. The arrows once again show the direction and magnitude of the current where, in contrast to Fig. 3, the length of the arrows is strictly proportional to $|\mathbf{j}|$. Figure 5 explains the appearance of the "forward" maximum in the absorption, whose presence is shown in Figs. 3 and 4. In this figure we show the geometrical path of rays refracted by the nucleus. The computation was done for 30-Mev neutrons (the wavelength for such neutrons is approximately 1.4 times greater than the wavelength for 18-Mev α particles, for which Figs. 3 and 4 were constructed). As we see from Fig. 5, the nucleus simply acts as a lens whose focus lies on the axis near the edge of the nucleus. The presence of this focus also explains the absorption maximum since, in the region of the focus, $|\Psi(\mathbf{r})|^2$ obviously has a maximum. Pic-

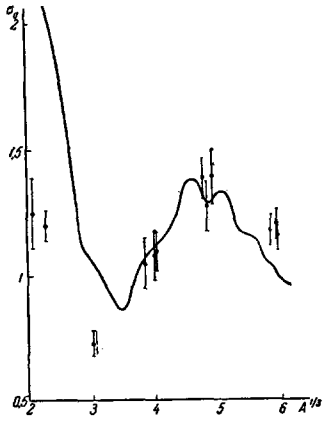

FIG. 6. Ratio $\sigma_b = \sigma_s/\sigma_t$ as a function of $A^{1/3}$. The solid curve is calculated from the optical model with a diffuse edge and volume absorption, for 14-Mev neutrons.

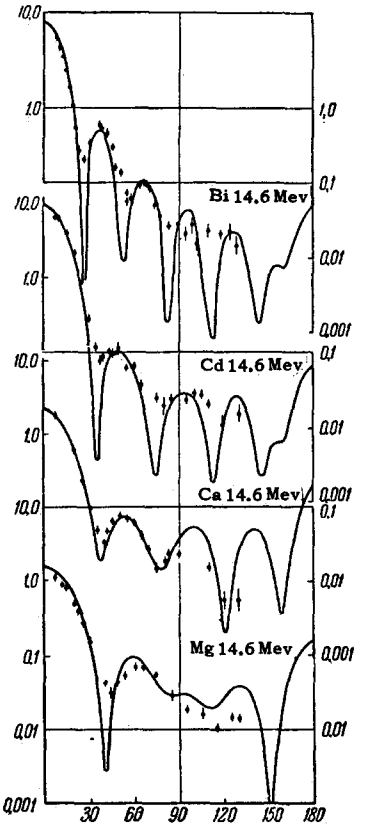

FIG. 7

$d\sigma_s/d\Omega$ for 14-Mev neutrons. The abscissa gives the scattering angle, and the ordinate gives $d\sigma_s/d\Omega$ in arbitrary units. The solid curves are the computations on the optical model with volume absorption and a diffuse edge.[6]

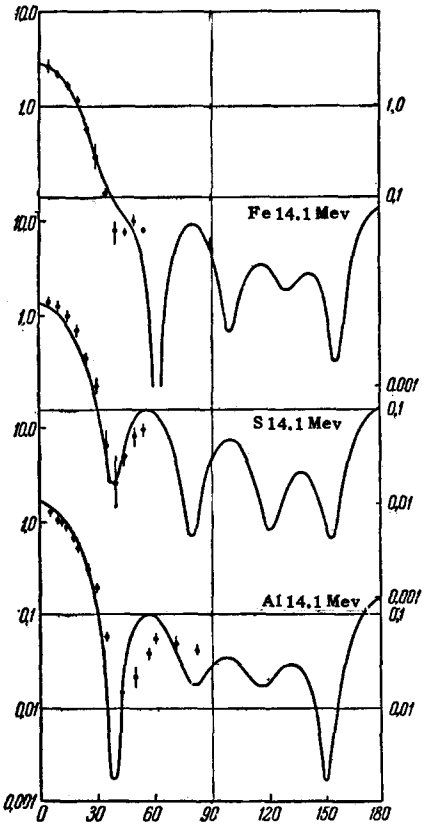

FIG. 8

tures of the type shown in Figs. 3, 4, and 5 may turn out to be very useful for understanding the dynamics of direct nuclear processes. The model of a nucleus with a diffuse edge and a volume central absorption still is not the best approximation to actuality. From a comparison of the computational data with the results of experiment one finds the following:

1. One can choose the parameters of the model to obtain good agreement of theoretical and experimental results for the total cross section σ_t and the value of σ_0 in the region of medium and heavy nuclei. But then the theoretical value of σ_0 for light nuclei is too high. Figure 6, taken from reference 6, which gives the scattering of neutrons with an energy of 14 Mev, illustrates this result.

2. The angular distribution of scattered neutrons is essentially described correctly by the model. However, one observes a discrepancy between the theoretical and experimental data on two counts:

a) The depth of the diffraction minima in the angular distribution is actually much less than one obtains from theory. (In other words, the theory predicts a much larger variation in intensity of scattered particles with change in angle of scattering ϑ than is actually the case);

b) The theory gives too high a value for the relative probability of scattering at angles close to 180°.

In Figs. 7 and 8, which are also taken from reference 6, one sees these differences very clearly. In these figures, the abscissa is the scattering angle and the ordinate is $d\sigma_S(\vartheta)$ in arbitrary units. The solid curves gives the theoretical results obtained with a potential defined by formulas (22) — (24) and (26). Entirely similar results are also obtained for a potential of the Woods-Saxon type.

The discrepancy between the theoretical and experimental data mentioned in Sec. 1 could also be eliminated by choosing for light nuclei a value of ζ approximately twice as large as for heavy nuclei. Such a marked "blackening of the nucleus" with decrease in A is, however, highly improbable. Therefore many authors, and in particular Fernbach and Bjorklund,[8] have introduced, for the purposes of improving the agreement of theory with experiment, a surface absorption, i.e., they have assumed that the imaginary part of the potential W(r) is different from zero only at the edge of the nucleus. With surface absorption, σ_0 should (for fixed values of the parameters in the potential) depend more weakly on the mass number of the nucleus than for the case of volume absorption, because the absorbing volume in the first case is equal (in order of magnitude) to $4\pi r_0^2 \bar{b} A^{2/3}$ (where $\bar{b}$ is the effective depth of the surface absorbing layer, which is independent of A), whereas it is $(4\pi/3) r_0^3 A$ in the second case. We should say immediately that there are no clear physical reasons for replacing the volume absorption by a surface absorption. Most usually, one gives as an argument in favor of the surface absorption the fact that, in the central region of the nucleus, for the most part those nucleons are neighbors which lie in the inner nucleonic shells, whose state is difficult to change because of the effect of the Pauli principle (since the higher states are occupied). Actually, however, as Peierls[9] has pointed out, this assertion is by no means correct, since there is no marked difference between the density of nucleons of the inner and outer shells in the central region of the nucleus.

Nevertheless, the introduction of surface absorption in the first place makes it possible to avoid the sharp jump in the imaginary part of the potential when we go from light nuclei to heavy nuclei (which, as we have pointed out, is necessary in the case of volume absorption for explaining the dependence of σ_0 on A), and, secondly, it eliminates the contradiction, pointed out in 2.a, between theory and experiment concerning the angular distributions (too deep diffraction minima in the theoretical curve in Fig. 7). The use of surface absorption improves the agreement of theory and experiment simultaneously in both respects, and thus justifies the increase in the number of parameters characterizing the optical potential which must be done when one introduces the surface absorption. In Bjorklund's calculations, the imaginary part of the potential was chosen as a Gaussian

$$W = W_0 e^{-(r-R)^2/b^2}, \tag{27}$$

where

$$\text{for neutrons} \quad b = 0{,}98 \cdot 10^{-13} \text{ cm}, \tag{28}$$

$$\text{for protons} \quad b = 1.2 \cdot 10^{-13} \text{ cm}. \tag{28a}$$

For 14-Mev neutrons,

$$W_0 = 7 \text{ Mev}. \tag{29}$$

In Table I we give data showing how well the computed values agree for a wide interval of values of σ_r, as obtained with the surface absorption model. The data given in the table refer to 14-Mev neutrons. The experimental results are those of MacGregor; the theoretical results are Bjorklund's (cf. reference 10).

For the real part of the potential Bjorklund used formula (20) with the parameter values (20a) and (21), where V_0 was taken to be equal to

$$V_0 = 44 \text{ Mev}. \tag{30}$$

As we see from the table, the dependence of σ_r on A over a wide interval of values from A = 9 to A = 209 is given extremely accurately by the results of the theoretical computation carried out using surface absorption. As already mentioned, the introduction of surface absorption enables us to eliminate the discrepancy between the theoretical and experimental results for the angular distribution which was pointed out in 2a. However, one does not succeed in eliminating the too high values of differential scattering cross section at angles close to 180° (2b).

Table I. Capture cross section σ_r for 14-Mev neutrons (in barns)

Element	Experiment	Theory	Element	Experiment	Theory
Be	0.51 ± 0.03	0.61	Cu	1.49 ± 0.02	1.47
B^{10}	0.66 ± 0.07	0.66	Zn	1.57 ± 0.03	1.48
C	0.56 ± 0.02	0.71	Zr	1.73 ± 0.03	1.75
F	0.88 ± 0.05	0.86	Ag	1.93 ± 0.03	1.85
Mg	1.00 ± 0.03	0.98	Cd	1.91 ± 0.03	1.90
Al	1.02 ± 0.02	1.04	Sn	1.89 ± 0.06	1.98
S	1.16 ± 0.06	1.04	Sb	1.96 ± 0.04	2.01
Ti	1.33 ± 0.03	1.34	Au	2.41 ± 0.04	2.48
Fe	1.34 ± 0.03	1.33	Hg	2.43 ± 0.03	2.49
Co	1.41 ± 0.03	1.40	Pb	2.56 ± 0.04	2.53
Ni	1.36 ± 0.02	1.35	Bi	2.56 ± 0.04	2.54

This point is related to the fact that up to now we have not taken into account the spin-orbit interaction of the impinging nucleons with the nucleus. Spin-orbit interaction leads first of all to a polarization of the scattered nucleon, and second, as will be shown later on, increases the relative intensity of nucleons scattered to the "side," i.e., at angles of the order of 90°.

c) Inclusion of spin-orbit interaction. Since the spin of the nucleon is $s = \frac{1}{2}$, its projection s_z on any given direction in space can take on only the two values $s_z = \pm \frac{1}{2}$. If this direction is physically distinguished in the process of scattering which we are considering, the nucleons with different spin projections on this physically distinguished direction may, in general, be scattered differently. This will occur, obviously, only if the forces of interaction between the nucleon and the nucleus depend on the orientation of the spin with respect to the possibly physically distinguished directions.

In the scattering process we deal with three physically distinguished directions

$$\mathbf{m} = \frac{\mathbf{k}+\mathbf{k}'}{2\cos\vartheta/2}, \qquad \mathbf{l} = \frac{\mathbf{k}-\mathbf{k}'}{2k\sin\vartheta/2}$$

and the normal to the plane of scattering*

$$\mathbf{n} = \frac{[\mathbf{k}\mathbf{k}']}{k\sin\vartheta}.$$

Let us examine which of these three directions in space might be important for spin effects. For this purpose we note first of all that, if the scattering depends on the orientation of the spin of the nucleon with respect to some direction, then we are actually dealing not with a single scattering amplitude, but with four amplitudes corresponding to the different values of s_z for the nucleon before and after the scattering. We shall denote the states (initial or final) with projection $s_z = +\frac{1}{2}$ by the index 1 and the states with projection $s_z = -\frac{1}{2}$ by the index 2. The scattering process is then described by four amplitudes which we shall denote by f_{11}, f_{22}, f_{12}, f_{21} (the first index is the initial state, the second denotes the final state). The first two amplitudes describe the scattering without change in spin orientation; the second pair of amplitudes corresponds to scattering with a change in s_z (called spin-flip scattering). Actually, we have a whole table of scattering amplitudes, i.e., a two-by-two matrix,

$$f = \begin{pmatrix} f_{11} & f_{12} \\ f_{21} & f_{22} \end{pmatrix}. \tag{31}$$

We note that any two-by-two matrix can be represented as a linear combination of four matrices:

the unit matrix

$$1 = \begin{pmatrix} 1 & 0 \\ 0 & 1 \end{pmatrix}$$

and the three Pauli matrices:

$$\sigma^{(1)} = \begin{pmatrix} 0 & 1 \\ 1 & 0 \end{pmatrix}, \quad \sigma^{(2)} = \begin{pmatrix} 0 & i \\ -i & 0 \end{pmatrix}, \quad \sigma^{(3)} = \begin{pmatrix} 1 & 0 \\ 0 & -1 \end{pmatrix}. \tag{32}$$

Thus we can write

$$f = \frac{1}{\sqrt{2}}\{a\cdot 1 + b_1'\sigma^{(1)} + b_2'\sigma^{(2)} + b_3'\sigma^{(3)}\} = \frac{1}{\sqrt{2}}\{a\cdot 1 + \mathbf{b}'\boldsymbol{\sigma}\}, \tag{33}$$

where a and b_i are functions of the scattering angle ϑ.

The differential scattering cross section at angle ϑ for fixed values of the spin in the initial and final states is obviously equal to

$$\frac{d\sigma_{\alpha\beta}}{d\Omega} = |f_{\alpha\beta}|^2 = \frac{1}{2}|(a\delta_{\alpha\beta} + \mathbf{b}'\boldsymbol{\sigma}_{\alpha\beta})|^2,$$
$$\delta_{\alpha\beta} = \begin{cases} 1, & \alpha=\beta, \\ 0, & \alpha\neq\beta. \end{cases} \tag{34}$$

If in an experiment we do not determine the spin orientations of the initial and final states, which is usually the case in experiments in which one measures the angular distribution of scattering, then to obtain the differential cross section measured by such an experiment we must sum (34) over all $\alpha, \beta = 1, 2$, i.e., over all orientations of the spin in the initial and final states:*

$$\frac{d\sigma_s(\vartheta)}{d\Omega} = \sum_{\alpha,\beta} |f_{\alpha\beta}|^2 = |a|^2 + |\mathbf{b}'|^2. \tag{35}$$

*$[\mathbf{k}\mathbf{k}'] = \mathbf{k}\times\mathbf{k}'$.

*Formula (35) is easily obtained if we note that

$$\sum_{\alpha,\beta} |f_{\alpha\beta}|^2 \operatorname{Sp} f^+ f = \frac{1}{2}\operatorname{Sp}\{(a\cdot 1 + \mathbf{b}'\boldsymbol{\sigma})(a^*1 + \mathbf{b}^*\boldsymbol{\sigma})\},$$

where Sp A denotes the sum of the diagonal elements of the matrix A: $\operatorname{Sp} A = A_{11} + A_{22}$, and we use the identities

$$\operatorname{Sp}\sigma_i\sigma_j = 2\delta_{ij}, \qquad \operatorname{Sp}\sigma_i = 0.$$

The value of $d\sigma_s/d\Omega$ should not change under rotations of the coordinate systems since it depends only on quantities which are invariant with respect to rotation —the angle ϑ between the two directions $\mathbf{k}$ and $\mathbf{k}'$ (in other words, on $\mathbf{k}\cdot\mathbf{k}'/k^2 = \cos\vartheta$) and the absolute value k of the wave vector. From this it follows that

$$|\mathbf{b}'|^2 \equiv |b_1'|^3 + |b_2'|^2 + |b_3'|^2 \text{ is invariant under rotation.} \tag{36}$$

But this means that the three functions $b_1'(\vartheta)$, $b_2'(\vartheta)$, and $b_3'(\vartheta)$ must be the components of a vector, since only a vector has the property (36). The vector $\mathbf{b}'$ can be directed only along one of the physically distinguished directions $\mathbf{m}$, $\mathbf{l}$, or $\mathbf{n}$. However, it is easy now to see that, since parity is conserved in nuclear interactions,

$$\mathbf{b}'(\vartheta) = b'(\vartheta)\,\mathbf{n}. \tag{37}$$

In fact, the conservation of parity means, in particular, that under a space inversion all the effective cross sections, including the cross section (34), remain unchanged. Since under an inversion $x \to -x$, $y \to -y$, $z \to -z$:

$$m_x \to -m_x, \quad m_y \to -m_y, \quad m_z \to -m_z, \tag{38}$$

$$l_x \to -l_x, \quad l_y \to -l_y, \quad l_z \to -l_z, \tag{39}$$

$$n_x \to +n_x, \quad n_y \to +n_y, \quad n_z \to +n_z, \tag{39'}$$

then, with the condition (37), the cross section (34) will be invariant under inversion. In fact, $a(\vartheta)$ and $b(\vartheta)$ are not changed under reflection since ϑ does not change and, according to (39'),

$$\mathbf{n}\sigma \to \mathbf{n}\sigma.$$

If the vector $\mathbf{b}'$ were directed along $\mathbf{m}$ or $\mathbf{l}$, then as a result of (38) the cross section (34) would change under an inversion, since

$$a\delta_{\alpha\beta} + b'\mathbf{m}\sigma_{\alpha\beta} \to a\delta_{\alpha\beta} - b'\mathbf{m}\sigma_{\alpha\beta},$$

which is possible only when parity is not conserved. From all this, it follows first of all that a possible distinguished direction for the spin orientation is the direction of the vector $\mathbf{n}$ normal to the scattering plane. This means that the scattering cross section can depend on the projections of the spins of the incident and scattered nuclei only along the direction $\mathbf{n}$. Secondly, from formulas (35) and (37) there follows the statement formulated in Sec. b of this paragraph concerning the reduction in the relative probability of scattering at angles close to 180°. In fact, it is clear that

$$b'(\vartheta)\,\mathbf{n}\sigma \to 0,$$

if $\vartheta \to 0$ or π, since for $\vartheta = 0$ or π the direction of the vector $\mathbf{n}$ becomes indeterminate, and if $\mathbf{b}'(\vartheta)\mathbf{n}\cdot\sigma$ went to zero at these angles, then we would obtain for the scattering amplitude at $\vartheta = 0$ and π physically meaningless expressions. Since

$$b'\mathbf{n} = \frac{[\mathbf{k}\mathbf{k}']}{k}\frac{b'}{\sin\vartheta},$$

it then follows that $b'/\sin\vartheta$ is finite for $\vartheta = 0$ or π. In other words we can write

$$b'(\vartheta) = b(\vartheta)\sin\vartheta, \tag{40}$$

where

$$|b| < \infty \quad \text{for} \quad \vartheta = 0 \quad \text{or} \quad \pi.$$

Then according to (36) and (37) we have

$$\frac{d\sigma_s(\vartheta)}{d\Omega} = |a|^2 + |b|^2\sin^2\vartheta. \tag{41}$$

If the scattering is independent of spin orientation, then

$$\frac{d\sigma_s(\vartheta)}{d\sigma_s(\vartheta_1)} = \frac{|a(\pi)|^2}{|a_1(\pi_1)|^2}, \qquad 0 \leqslant \vartheta_1 \leqslant \pi. \tag{42}$$

If the nuclear potential depends on the spin orientation, then according to (40) we have

$$\frac{d\sigma_s(\pi)}{d\sigma_s(\vartheta_1)} = \frac{|a(\pi)|^2}{|a(\vartheta_1)|^2 + |b(\vartheta_1)|^2\sin^2\vartheta_1}. \tag{43}$$

Thus we see that the dependence of scattering on spin orientation of the nucleon leads to a reduction in the relative probability of scattering at angles close to 180°. The same situation exists for scattering angles close to 0. [The magnitude of the effect still depends, of course, on the behavior of $b(\vartheta)$ as a function of ϑ.]

It is easy to see that at the same time the total cross section remains unchanged, since, according to formula (12), σ_t is expressed in terms of the forward scattering amplitude. From this it also follows that the spin-dependence of the scattering has very little effect on the magnitudes of the first, most intense, diffraction maxima and minima. In fact, let us consider the scattering by a real potential. In this case $\sigma_t = \sigma_s$, and consequently σ_t is not changed by the introduction of forces which depend on the orientation of the spin relative to $\mathbf{n}$. But the quantity σ_s is determined for the most part by the area of the first few diffraction maxima, by their heights and extension. Since σ_s is not changed, these quantities also cannot change essentially.* It is therefore clear that the spin dependence of the scattering affects the angular distribution only at large angles. This situation remains when we have a complex potential. Thus, the dependence of the potential on the orientation of the spin of the nucleon practically changes neither σ_s nor σ_r, since the contribution of the higher diffraction maxima to σ_s at nucleon energies of the order of 10 Mev amounts to only a few percent. (this is much smaller than the experimental errors in the measurements of σ_s and σ_r), but can give a significant change in the angular distribution of the scattered nucleons at angles close to π (namely, decrease the relative intensity of scattering at angle π) which, as we saw in the preced-

*This assertion is, of course, valid in those cases where the angular distribution is sufficiently strongly peaked forward, i.e., for nucleon energies above 5 Mev.

ing sections, is just what is required to give agreement between the theoretical and experimental results.

If the scattering is dependent on spin orientation, this may lead to the result that the scattered nucleons are polarized in a direction ν, even if the incident nucleons are unpolarized. Let us express the polarization of the nucleons in terms of the amplitudes $f_{\alpha\beta}$. By the polarization P_ν we mean the quantity

$$P_\nu = \frac{J_+ - J_-}{J_+ + J_-} = \frac{d\sigma_+ - a\sigma_-}{d\sigma_s}, \tag{44}$$

where J_+ and J_- are the numbers of nucleons scattered at angle ϑ with projection s_z on the direction ν, equal respectively to $\pm\frac{1}{2}$; $d\sigma_+$ and $d\sigma_-$ are the differential scattering cross sections corresponding to these nucleon spin orientations in the final state. According to the preceding statements,

$$d\sigma_+ = \{|f_{11}|^2 + |f_{21}|^2\}\Omega, \tag{45}$$

$$d\sigma_- = \{|f_{22}|^2 + |f_{12}|^2\}d\Omega. \tag{46}$$

We now note that it follows from (33) that

$$|f_{12}|^2 = |f_{21}|^2. \tag{47}$$

Since

$$f_{12} = \frac{b}{\sqrt{2}} \sin\vartheta \cdot \sin\theta e^{i\varphi}, \tag{48}$$

$$f_{21} = \frac{b}{\sqrt{2}} \sin\vartheta \cdot \sin\theta e^{-i\varphi}, \tag{49}$$

where θ and φ are the polar angles of the vector $\mathbf{n}$ ($Oz \parallel \nu$). Thus

$$d\sigma_+ - d\sigma_- = \{|f_{11}|^2 - |f_{22}|^2\}d\Omega. \tag{50}$$

But for f_{11} and f_{22} we have the equations

$$f_{11} = \frac{a + b_3'}{\sqrt{2}}, \quad f_{22} = \frac{a - b_3'}{\sqrt{2}}, \tag{51}$$

where

$$b_3' = b \sin\vartheta \cdot \cos\theta = b \sin\vartheta\, \mathbf{n}\nu, \tag{52}$$

since $\nu \parallel Oz$.

Substituting (51) and (52) in (50) and using formula (35) for $d\sigma_S(\vartheta)$, we obtain:

$$P_\nu(\vartheta) = P(\vartheta)\mathbf{n}\nu, \qquad P(\vartheta) = \frac{ab^* + a^*b}{|a|^2 + |b|^2 \sin^2\varphi} \sin\vartheta. \tag{53}$$

From formula (53) it is clear that the polarization $P_\nu(\vartheta)$ goes to zero for $\vartheta = 0$ and π. This is also to be expected since at $\vartheta = 0$ or π the physically distinguished direction, the direction of the vector $\mathbf{n}$, ceases to be determinate. An important conclusion which follows from the above statement is that if we introduce a nuclear potential depending on spin orientation for the purpose of obtaining the correct behavior of the angular distributions at angles ϑ close to π, then this same potential must give values of the polarization $P_\nu(\vartheta)$ of the scattered nucleons in accord with experiment.

Now let us see what the form of the potential which depends on the nucleon spin orientation should be. As already discussed above, in this case we must treat two wave functions $\psi_1(r)$ and $\psi_2(r)$ corresponding to the two orientations of the nucleon spin before the scattering. For $r \to \infty$ these functions will have the form

$$\psi_1(\mathbf{r})_{r\to\infty} = \frac{1}{\sqrt{2}} e^{-ikr} + (f_{11} + f_{12})\frac{e^{ikr}}{r}, \tag{54}$$

$$\psi_2(\mathbf{r})_{r\to\infty} = \frac{1}{\sqrt{2}} e^{ikr} + (f_{22} + f_{21})\frac{e^{ikr}}{r}. \tag{55}$$

Neither these functions themselves nor linear combinations of them can be solutions of two independent equations since $|f_{12}|^2 = |f_{21}|^2 \neq 0$.* Therefore in place of the Schrödinger equation (1) we must write a system of two differential equations with four potentials U_{11}, U_{12}, U_{21}, and U_{22}:

$$\begin{aligned}(\nabla^2 + k^2)\psi_1 - \tfrac{2m}{\hbar^2}(U_{11}\psi_1 + U_{12}\psi_2) = 0,\\ (\nabla^2 + k^2)\psi_2 - \tfrac{2m}{\hbar^2}(U_{22}\psi_2 + U_{21}\psi_1) = 0,\end{aligned} \tag{56}$$

or in matrix form

$$\left\{\nabla^2 + k^2 - \frac{2m}{\hbar}\hat{U}(r)\right\}\Psi = 0, \tag{56a}$$

where

$$\hat{U} = \begin{pmatrix} U_{11} & U_{12} \\ U_{21} & U_{22} \end{pmatrix} \tag{57}$$

is the matrix of the potential and

$$\Psi = \begin{pmatrix} \psi_1 \\ \psi_2 \end{pmatrix} \tag{58}$$

denotes the two-component wave function of the nucleon. Using the properties of the Pauli matrices, we write

$$U(\mathbf{r}) = U(\mathbf{r})\cdot 1 + \frac{1}{2}\mathbf{U}_s\sigma. \tag{59}$$

The vector $\mathbf{U}_S$ can be directed only along the vectors $\mathbf{r}$, ∇, or $[\nabla \times \mathbf{r}]$ which are available to us. In exactly the same way as in establishing the form of the matrix of the scattering amplitudes from conservation of parity, i.e., from the invariance of $\hat{U}_{\alpha\beta}$ with respect to space inversion, it follows that

$$\mathbf{U}_s = V_s'(r)[\nabla\mathbf{r}], \tag{60}$$

or, introducing the orbital angular momentum operator (in units of $\hbar$)

$$\hat{\mathbf{l}} = -i[\nabla\mathbf{r}], \tag{61}$$

we obtain

$$\mathbf{U}_s = V_s(r)\hat{\mathbf{l}}, \tag{62}$$

where

*If $f_{12} = f_{21} = 0$, the functions

$$\frac{1}{\sqrt{2}}(\psi_1 + \psi_2)_{r\to\infty} = e^{ikr} + a\frac{e}{r}^{ikr},$$

$$\frac{1}{\sqrt{2}}(\psi_1 - \psi_2)_{r\to\infty} = b\sin\vartheta\, \mathbf{n}\nu\frac{e}{r}^{ikr}$$

could be solutions of two independent equations since a and b are independent.

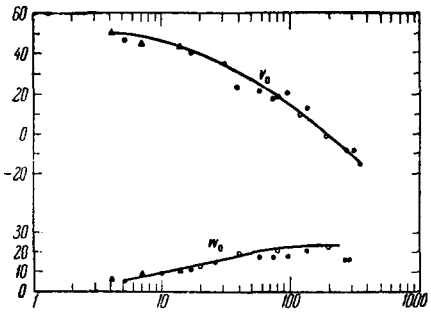

FIG. 9. Dependence of V_0 (upper curve) and W_0 on nucleon energy (abscissa in Mev) in a model with surface absorption and diffuse edge (for V we use the Woods-Saxon potential, for W a Gaussian curve). The values of V_0 and W_0 (ordinates) are given in Mev.

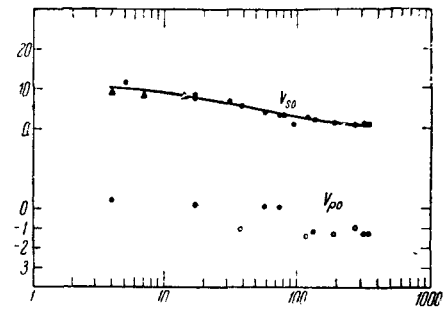

FIG. 10. Dependence of spin-orbit potential on nucleon energy. Upper curve – real part of V_{s0} in Mev, lower points – imaginary part $V_{\rho 0}$.

$$V_s(r) = iV_s'(r).$$

Thus the matrix potential $\hat{U}(r)$ takes the form

$$\hat{U}(\mathbf{r}) = U(r)\cdot 1 + V_s(r)\cdot \hat{\mathbf{l}}\hat{\mathbf{s}}, \qquad \mathbf{s} = \frac{1}{2}\sigma. \tag{63}$$

Here $U(r)$ is the usual central potential treated by us earlier. The second term in (63) describes the spin-orbit interaction. The form of the spin-orbit potential $V_S(r)$ cannot be established from general physical considerations. Good agreement with the experimental data is obtained if we choose $V_S(r)$ in a form analogous to the atomic spin-orbit potential

$$V_s = V_{s0}\left(\frac{\hbar}{\mu c}\right)^2 \frac{1}{r}\frac{df}{dr}, \tag{64}$$

where $V_{S0} > 0$ and $f(r)$ is a function which determines the dependence of the real part of the potential $V(r)$ on r. The quantity $\hbar/\mu c = 1.4 \times 10^{-13}$ cm is the Compton wavelength of the π meson (μ is the rest mass of the π meson), which is introduced into (64) purely formally to make V_{S0} have the dimensions of an energy. In the case of the Woods-Saxon potential, for example,

$$\frac{df}{dr} = -\frac{1}{a}\frac{e^{(r-R)/a}}{(1+e^{(r-R)/a})^2}. \tag{65}$$

Up to energies of the order of 100 Mev, the experimental data are well described on the assumption that V_{S0} is a real quantity. Thus the spin-orbit potential in the form (64) is determined by a single constant. Frequently V_{S0} is written in the form

$$V_{s0} = \varkappa\left(\frac{\mu c}{\hbar}\right)^2 V_0,$$

where the constant of the spin-orbit coupling κ has the dimensions cm^2.

d) Comparison of theoretical and experimental results. In comparing the experimental data with the results of computations on the optical model, one must keep in mind (especially for energies of the order of 1 Mev) that the theoretical values of σ_S should be somewhat lower than the experimental results. This is related to the fact that, in the optical model, resonance scattering, i.e., scattering which proceeds via the formation of a compound nucleus with its subsequent decay, in which a nucleon is emitted with an energy precisely equal to the initial energy, is contained in the quantity σ_r and not in σ_S.

However, resonance scattering is quite improbable if the compound nucleus is formed in a state with sufficiently high excitation energy, so that there are many different paths available for its decay (many "open channels"). Such a situation actually already occurs in practice in most cases for energies of the incident particles above 2 or 3 Mev.

We shall consider for the most part a model with a diffuse edge, surface absorption, and the spin-orbit potential (64) (results for a model with volume absorption are described in detail in the monograph of Nemirovskii[11]). The most detailed calculations of this sort are those of Fernbach and Bjorklund,[8] who used for $V(r)$ the Woods-Saxon potential and for $W(r)$ formula (27). For the parameters a, b, R, they chose the values (20a), (21), and (28). In Fig. 9 are shown the dependence on nucleon energy of the quantities V_0 and W_0. As we see from Fig. 9, V_0 falls off and W_0 increases with increasing energy, as should be expected since the greater the energy of the incident nucleons, the less the effect of the Pauli principle in limiting the number of possible states of the colliding particles (impinging particle and nucleon in the nucleus). We note that although in Fig. 9 the dependence of W_0 on E is shown up to an energy of the order of 100 Mev, the surface absorption actually is in good agreement with experimental data up to energies of the order of 50 Mev. For larger energies of the incident nucleons, the best agreement with experiment seems to be obtained in the model with volume absorption. In Fig. 10 is shown the dependence of the spin-orbit potential V_{S0} on energy (upper curve). The lower curve refers to the imaginary part of the spin-orbit potential. Here the data are less definite, although it appears to be clear that up to an energy of the order of 40 Mev at least, the imaginary part of the spin-orbit potential is equal to zero.

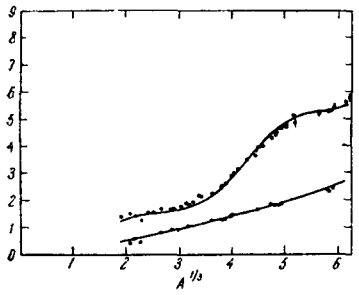

FIG. 11. σ_t (upper curve, in barns) and σ_r as functions of $A^{1/3}$ for 14-Mev neutrons. The solid curve is a computation for a model with diffuse edge and surface absorption.

The dependence shown in Figs. 9 and 10 is quite well approximated by the following formulas (for E $\lesssim$ 15 Mev):

$$V_0 = 52{,}5 - 0.6E \text{ Mev}, \quad (66)$$

$$W_0 = 2.5 + 0.3E \text{ Mev}, \quad (67)$$

$$V_{s0} = 10.0 - 0.15E \text{ Mev}. \quad (68)$$

As we see from (68), when E = 14 Mev, V_{S0} is equal to 8 Mev, which corresponds to $\kappa \simeq 3.5 \times 10^{-27}$ cm^2. (This constant was first established by Levintov.[12]) Figures 11 and 12 show the neutron cross section σ_t (upper curves) and σ_r (lower curves) as functions of mass number A. These data indicate the very good agreement of theory with experiment over a wide interval of values of A from 8 up to 200. In Fig. 13 we give curves of $d\sigma_S(\vartheta)$ for 14-Mev neutrons. These curves also show the excellent agreement of theory and experiment (except, possibly, for the data on scattering by Al). In this figure an interesting point is the absence of deep minima which are characteristic for the model with volume absorption, and the beautiful agreement of the theoretical and experimental data for scattering at angles close to π, which, as pointed out above, is a consequence of the inclusion of spin-orbit coupling.

In Fig. 14 we give curves of polarization of scattered neutrons (E = 3.1 Mev) as a function of scattering angle ϑ. The experimental data were obtained as usual by observing the azimuthal asymmetry in double scattering. As one sees from Fig. 14, there is no agreement between the theoretical and experimental results; the situation is especially bad in the case of lead and tin. The reason for the discrepancy is still not clear, and this question requires additional (experimental and theoretical) investigation.

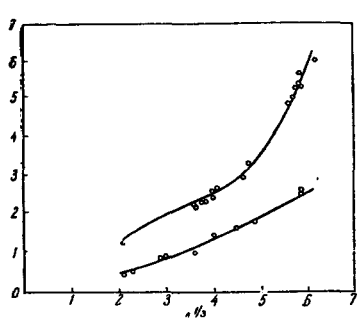

FIG. 12. σ_t (upper curve, in barns) and σ_r as a function of $A^{1/3}$ for 26-Mev neutrons. See remarks for Fig. 11.

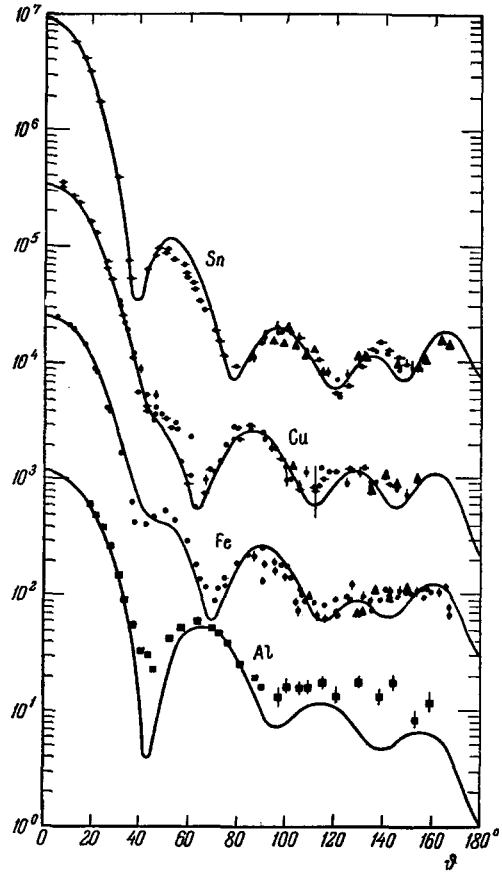

FIG. 13. $d\sigma_s/d\Omega$ (mb/sr) for 14-Mev neutrons. The scatterers are tin, copper, iron, and aluminum.

It should be mentioned that for high-energy neutrons and protons the agreement of theoretical and experimental results on polarization in the model with surface absorption is entirely satisfactory. Such a conclusion follows, for example, from the analysis of data on polarization of 8.5- and 10.5-Mev protons scattered by various nuclei (from Be to Ag, cf. reference 13). The theoretical results obtained on the basis of the optical model give essentially the correct absolute values of $P(\vartheta)$, as well as the dependence of the degree of polarization on the scattering angle ϑ. In particular, the experiments confirm the prediction of the optical model that there is a systematic decrease in polarization with increasing A. Another confirmation of the diffraction nature of the polarization phenomena (i.e., the fact that the difference in scattering cross sections for particles with different spin orientations can be described by a spin-orbit potential) is the fact that the location of the maxima and minima in the polarization is, in first approximation, a function only of the quantity

$$\eta = |\mathbf{k} - \mathbf{k}'| R = 2kR \sin\frac{\vartheta}{2},$$

as should be the case for Fraunhofer diffraction by a homogeneous obstacle of radius R.

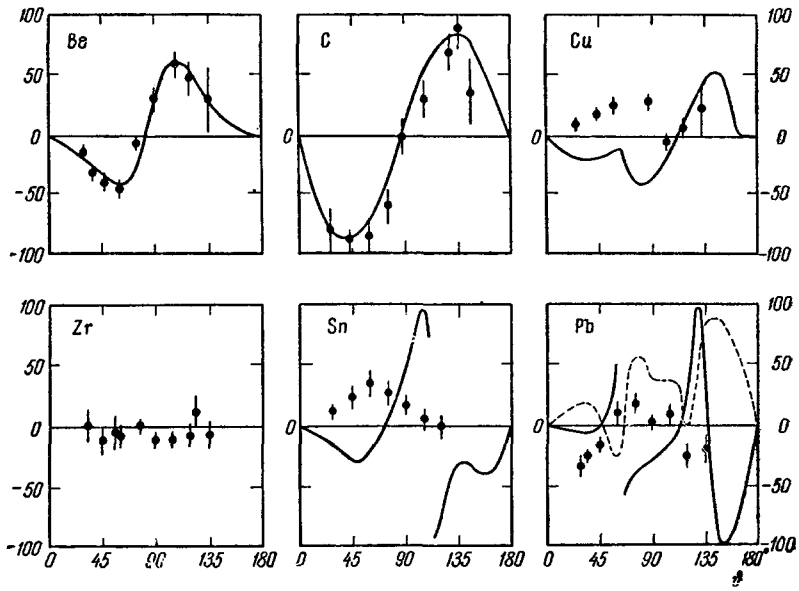

FIG. 14. Polarization of neutrons P(ϑ) (in %) as a function of ϑ for 3.1-Mev neutrons. The solid curves are computations on the optical model with diffuse edge and surface absorption.

This circumstance is illustrated by Fig. 15 in which is shown the value of η for the maxima and minima in the polarization of nucleons with an energy around 10 Mev, scattered by various nuclei. As one sees from the figure, the value of η is approximately constant for maxima and minima of the polarization over a wide range of variation of A.

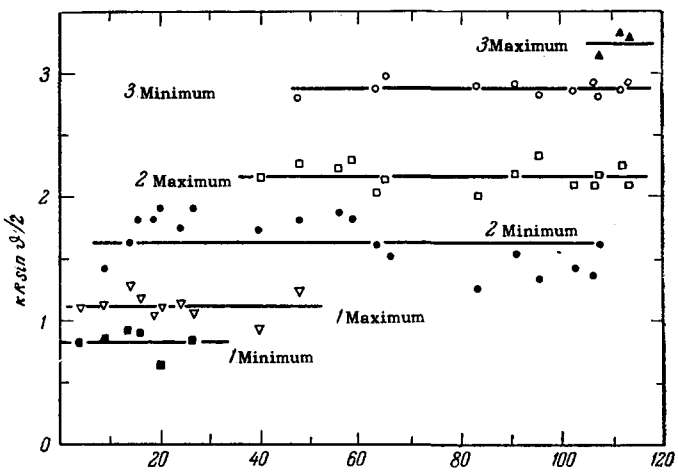

FIG. 15. Values of kRsin(ϑ/2) for maxima and minima in the polarization P(ϑ) as a function of mass number A.

We have already remarked concerning the results obtained in the model with volume absorption. The defects of this model which were pointed out in Sec. 3 make it preferable, for E < 50 Mev, to use the model with surface absorption.

However, in certain cases, even with volume absorption, one can obtain satisfactory agreement with experiment, though the parameters of the potential must then be allowed to vary markedly as we go from nucleus to nucleus. As an example of this, we may cite the data shown in Figs. 16 and 17. In these figures are shown curves of P(ϑ) and $d\sigma_S(\vartheta)$ for 10-Mev protons,[14] scattered by nitrogen and argon nuclei. As we see from the data shown in the graphs, the quantities V_0, W_0, V_{S0} and a, even though they change when we go from nitrogen to argon, have approximately the same order of magnitude as in the model with surface absorption.

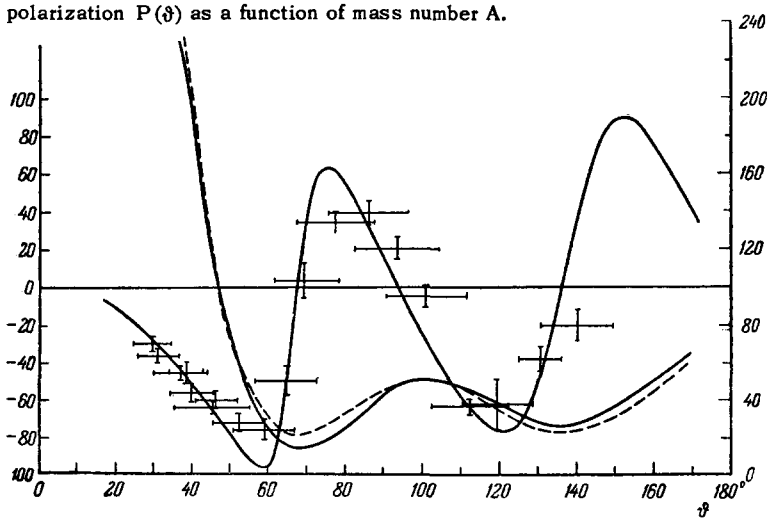

FIG. 16. Polarization P(ϑ) (left scale, in %) and $d\sigma_s/d\Omega$ (right-hand scale, mb/sr) as functions of scattering angle ϑ (in the c. m. system) for 10-Mev protons (scattering by nitrogen nuclei). The solid curves are for a model with diffuse edge and volume absorption; the dashed curve is the experimental data for $d\sigma_s/d\Omega$. The parameters are: r_0 = 1.2 fermi, a = 0.6 fermi, V_0 = 0.49 Mev, W_0 = 3.0 Mev, V_{S0} = 10.0 Mev.

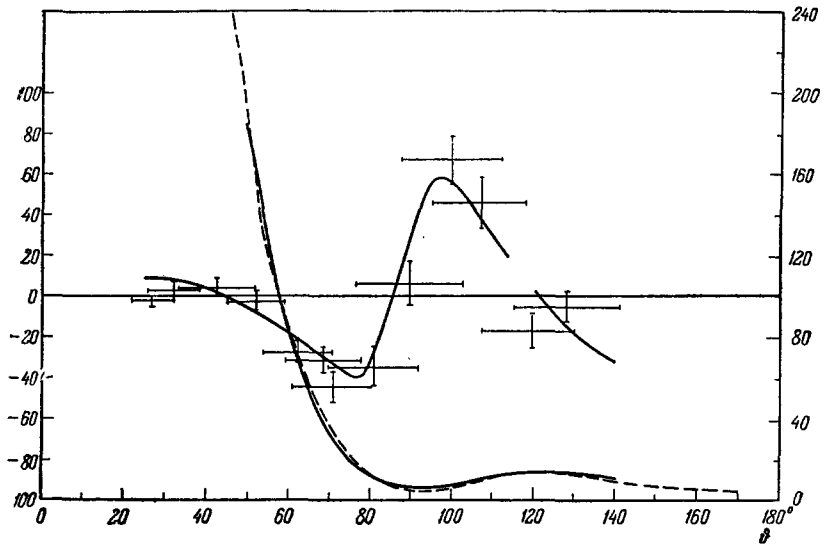

FIG. 17. Polarization $P(\vartheta)$ (left scale, in %) and $d\sigma_s/d\Omega$ (right-hand scale, mb/sr) as functions of scattering angle ϑ (in the c. m. system) for 10-Mev protons. The scatterer was argon. The notation is the same as in Fig. 16. The parameters are: $r_0 = 1.2$ fermi, $a = 0.415$ fermi, $V_0 = 61.76$ Mev, $W_0 = 8.78$ Mev. $V_{s0} = 20$ Mev.

II. THE OPTICAL MODEL FOR SCATTERING OF COMPOSITE PARTICLES

3. Scattering of α particles

In recent years it has become clear that, just as for the case of nucleons, in the scattering of α particles we cannot treat the nucleus as a black body.

We know that for α particle energies below the Coulomb barrier for a given nucleus the scattering occurs almost entirely as Rutherford scattering. The same situation remains for energies above the Coulomb barrier, but for small scattering angles. This is explained by the fact that the cross section for Rutherford scattering at small angles is large, since it can occur even when the α particle passes far from the nucleus.

The non-electromagnetic, nuclear interaction of the α particle and the nucleus manifests itself mainly for scattering at large angles. For the reasons cited, quantitative conclusions concerning "nuclear" (non-electromagnetic) scattering of α particles became possible only after experiments were done in which scattering was observed at large angles for α particles which were accelerated artificially to high energies (of the order of 30 Mev and more). For these energies the α-particle wavelength is $\lambda \ll R$, which is an essential point for what follows. Let us first of all consider the results of the theory in which the nucleus is regarded as being "black" for α particles.

In this case the smallness of the wavelength of the α particle permits us to simplify considerably the treatment of the nuclear Coulomb field.

As already pointed out above, for $\lambda \ll R$, diffraction (wave) phenomena, appear only at distances of the order of or greater than R^2/λ. Near the nucleus the picture will be practically the same as that of "geometrical optics," i.e., the α particles will move along classical trajectories. In this case, these trajectories will not be straight lines, as they would be for uncharged particles, but hyperbolas, since the Coulomb field of the nucleus acts on the α particles. The latter is a slowly-varying function of r, and at distances of the order of λ changes only insignificantly. Therefore, the motion of α particles in the Coulomb field can be treated as classical. The presence of a black absorbing nucleus has the result that, at distances greater than R^2/λ, one gets a diffraction picture whose optical analogue is the diffraction of light by a black sphere placed in a medium with a slowly varying index of refraction (varying as $\sqrt{1-a/r}$, where r is the distance from the center of the sphere). We recall that, in contrast to this, the scattering of neutrons corresponded to a picture of diffraction of light by a black sphere in a homogeneous medium with a constant index of refraction. In practice, the computation of $d\sigma_S(\vartheta)$ for α particles on this scheme is carried out as follows: if, as usual, we expand the scattering amplitude in partial waves with given orbital angular momentum:

$$f(\vartheta)=\frac{i\sqrt{\pi}}{k}\sum\sqrt{2l+1}(1-f_l)P_l(\cos\vartheta), \qquad (69)$$

where $P_l(\cos\vartheta)$ are Legendre polynomials and f_l are the amplitudes of the scattered partial waves, independent of ϑ, then for l greater than some value l', the f_l are exactly equal to the amplitudes of the waves scattered by a "pure" Coulomb field, (i.e., in the absence of the black nucleus) while for $l \leq l'$

$$f_l = 0. \qquad (70)$$

In fact, from the classical point of view ("geometrical optics" in the neighborhood of the nucleus) only those particles can penetrate into the nucleus for which the energy E is greater than the sum of the heights of the Coulomb barrier U_k and the centrifugal barrier U_l. Since

$$U_k=\frac{2Ze^2}{R}, \qquad (71)$$

$$U_l=\frac{\hbar^2 l(l+1)}{2m_\alpha R^2}, \qquad (72)$$

the condition

$$E=\frac{2Ze^2}{R}+\frac{\hbar^2 l'(l'+1)}{2m_\alpha R^2} \tag{73}$$

determines the maximum orbital angular momentum l' of particles which can penetrate into the nucleus.

If $l \ll l'$, the wave penetrates into the nucleus and is absorbed there (the nucleus is black), so that the amplitude f_l for such partial waves should be set equal to zero. If, however, $l > l'$, the wave does not penetrate into the nucleus and only the Coulomb field acts on it, so that f_l for $l > l'$ is not affected by the presence of the black absorbing nucleus. These statements can be understood by noting that, for neutrons, (73) goes over into the condition

$$E=\frac{\hbar^2 l'^2}{2mR^2} \quad (l' \gg 1), \tag{74}$$

which can be rewritten as

$$l'=\frac{R}{\lambda\!\!\!^{-}}, \quad \lambda\!\!\!^{-}=\frac{\hbar}{\sqrt{2mE}}. \tag{75}$$

This last condition, if we introduce the impact parameter d (i.e., the distance from the nucleus to the classical trajectory of the particle, which in the case of neutrons is a straight line—the "rays" of geometrical optics in a homogeneous medium), can be expressed as

$$d=R, \tag{76}$$

since $l' = dp/\hbar$, where $p = \sqrt{2mE}$ is the neutron momentum. Thus the condition for penetration into the nucleus, $l \leq l'$, is simply the trivial geometrical condition for "shadow" and "illumination,"

$$d \leqslant R. \tag{77}$$

The presence of the Coulomb field changes the condition (77) in exactly the same way as the index of refraction of light in the medium with an index which varies according to the law $\sqrt{1-a/r}$, "shifts" the light from the sphere whose center is located at the point r = 0. Therefore the region of geometrical shadow right near the sphere (far from it we have a diffraction picture) still remains: only those rays which are close to the normal to the sphere surface are not refracted and impinge on the surface of the sphere and are absorbed by it. The model described above for α particle scattering was first treated by Blair[15] and has been given the name of the "sharp cut-off model" in the foreign literature. We shall call it the black nucleus model. The characteristic results for the black nucleus model are shown in Fig. 18 which is taken from Blair.[16] In this figure, the dashed curve shows the results of a computation of the ratio $d\sigma_S(\vartheta)/d\sigma_R$ (where $d\sigma_R$ is the Rutherford scattering cross section) for the scattering of 48.2 Mev α particles by gold. In this case ($l' = 22$) R was set equal to 1.3×10^{-12} cm (which is somewhat greater than the radius of this nucleus for neutrons, which is approximately 0.73×10^{-12} cm).

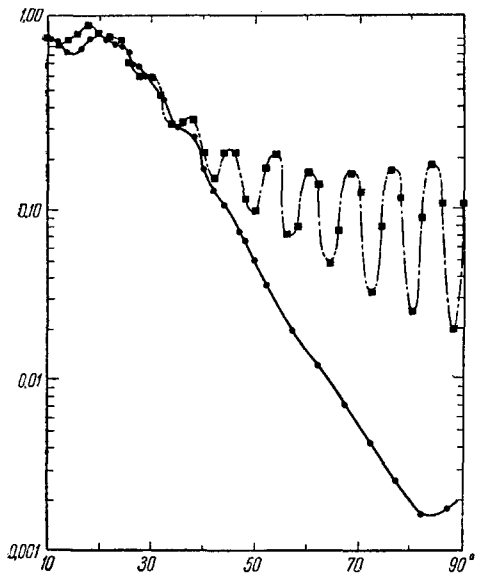

FIG. 18. $d\sigma_s/d\sigma_R$ for 48.2-Mev α particles. The scatterer is Au^{197}. The abscissa gives the scattering angle ϑ. The dashed curve is a computation on the black nucleus model; the solid curve gives the experimental data.

The solid curve in Fig. 18 is drawn through the experimental points. As we see from the figure, starting with scattering angles $\vartheta \simeq 40°$, the experimental data and the results of the theoretical computations disagree markedly. (For $\vartheta = 90°$ the theoretical values are 50 times greater than the experimental results.) This shows convincingly that the black nucleus model is unsuitable for describing α-particle scattering.

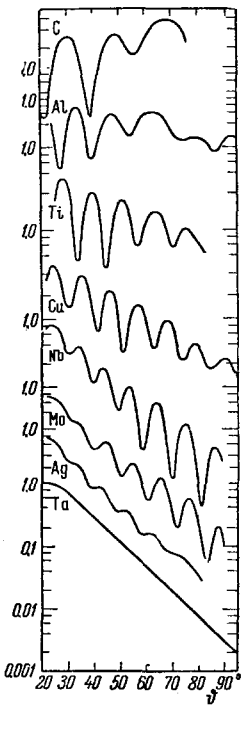

FIG. 19. Experimental data on the angular distribution of scattering of 40.2-Mev α particles by various nuclei. The abstcissa is the scattering angle ϑ (in the c. m. system); the ordinates are $d\sigma_s/d\sigma_R$.

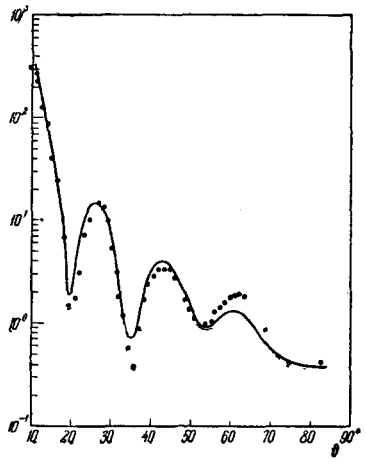

FIG. 20. $d\sigma_s/d\Omega$ (mb/sr) for 40.2-Mev α particles. The scatterer is carbon. The solid curve is computed on the optical model (ϑ in the c. m. system).

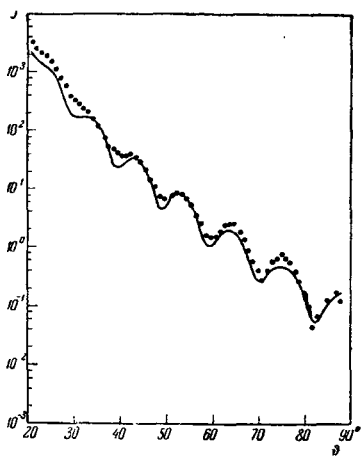

FIG. 22. $d\sigma_s/d\Omega$ (mb/sr) for 40.2-Mev α particles. The scatterer is Mo. The solid curve is computed on the optical model (ϑ in the c. m. system).

Nevertheless, the optical model with a diffuse edge, and not assuming the nucleus to be black, is in good agreement with the experimental data, and gives an almost exact description of the details of the angular distribution. In Fig. 19 is shown the general form of the curves for the ratio $d\sigma_S/d\sigma_R$ as a function of scattering angle ϑ, obtained in various experiments. As we see from the figure, these curves, which oscillate for light and medium heavy nuclei, become monotonic for heavy nuclei. The calculations, carried out by Igo and Thaler[17] using an optical model with diffuse edge and volume absorption, reproduce very closely the behavior of the experimental curves for all A. As an example, we shown in Figs. 20 — 23 a comparison of the results of Igo and Thaler with the experimental data on scattering of 40.2-Mev α particles from C, Ti, Mo, and Au nuclei. The authors of this paper used the Woods-Saxon potential with the following parameters:

$$R=(1{,}35\cdot A^{1/3}+1{,}3)\cdot 10^{-13}\ \text{cm}, \tag{78}$$

$$a=0.5\cdot 10^{-13}\ \text{cm}, \tag{79}$$

$$V_0=30-51\ \text{Mev}, \quad W_0=9-13\ \text{Mev}. \tag{80}$$

These values of the parameters refer to an energy of E = 40.2 Mev. In going from nucleus to nucleus the parameters are changed somewhat (mainly V_0), where the smallest value V_0 = 30 Mev applies to the light nuclei C, Al, and Ti. In the wide interval Cu-Th, V_0 = 47 — 51 Mev. Approximately the same results were obtained in a paper by Cheston and Glassgold.[18]

In all probability, one could achieve even better agreement with experiment and more constant values of the parameters as functions of A in a model with surface absorption. If we calculate, using (80), the mean free path Λ of α particles in the Au nucleus, we get

$$\Lambda_\alpha=2\cdot 10^{-13}\ \text{cm},$$

which is ten times greater than the mean free path of a nucleon with an energy of the order of 10 Mev in a black nucleus [cf. formula (10a)].

4. Scattering of Deuterons

A still more surprising effect is the transparency of nuclei for 10 — 15 Mev deuterons. In Figs. 24, 25, and 26 we give experimental data ($d\sigma_S/d\sigma_R$ as a func-

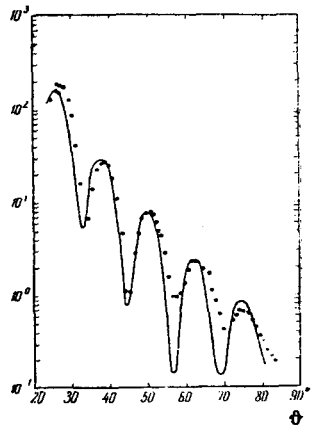

FIG. 21. $d\sigma_s/d\Omega$ (mb/sr) for 40.2-Mev α particles. The scatterer is Ti. The solid curve is computed on the optical model (ϑ in the c. m. system).

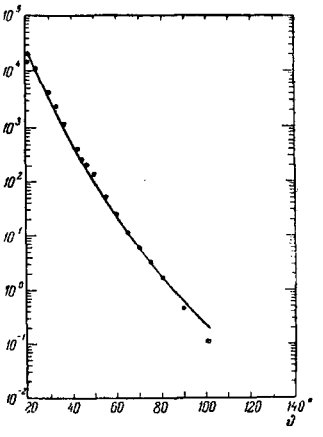

FIG. 23. $d\sigma_s/d\Omega$ (mb/sr) for 40.2-Mev α particles. The scatterer is Au. The solid curve is computed on the optical model (ϑ in the c. m. system).

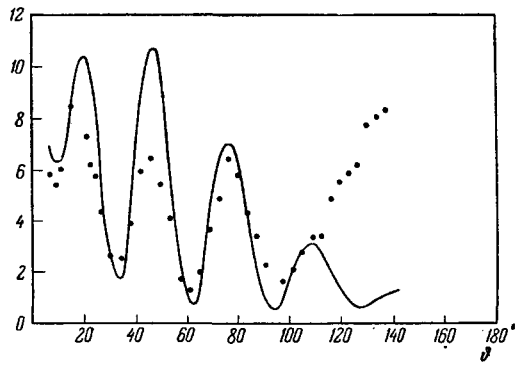

FIG. 24. $d\sigma_s/d\Omega$ for 15-Mev deuterons. The scatterer was Al. The solid curve gives computations on the optical model with volume absorption (ϑ in the c. m. system).

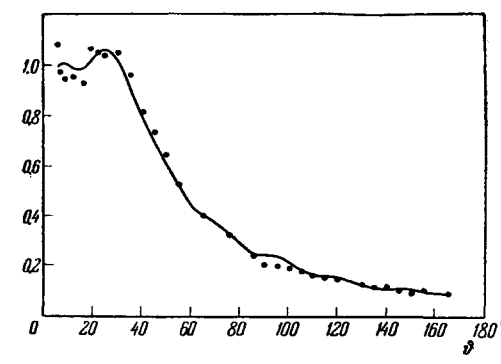

FIG. 26. $d\sigma_s/d\Omega$ for 15-Mev deuterons. The scatterer was Au. The solid curve gives computations on the optical model with volume absorption (ϑ in the c. m. system).

tion of scattering angle ϑ) for the scattering of 15 Mev deuterons by Al, Rh, and Au nuclei, as well as theoretical curves obtained on the basis of the optical model with a diffuse edge and volume absorption (Woods-Saxon potential).

In Table II we give the optical potential parameters.[19] The mean free path calculated, using these parameters, for 15-Mev deuterons in a gold nucleus is approximately equal to half the nuclear radius $\Lambda_D \simeq 4 \times 10^{-13}$.

The very good agreement of the theoretical results obtained on the basis of the optical model with the experimental data is unexpected because the "loose" structure of the deuteron (low binding energy) allows it to be deformed at quite large distances from the nucleus. This occurs in principle because of two effects: the action of the Coulomb field and the distortion of the wave front as a result of diffraction. The latter phenomenon is especially important for diffraction at large angles where the deuteron momentum changes a great deal:

$$\Delta p = |\mathbf{p} - \mathbf{p}'| \simeq 2p.$$

When there is a change in the momentum of the center of gravity, each of the nucleons constituting the deuteron can obtain a velocity relative to the center of gravity of the order of $\Delta p/m_D$, and consequently has, in the reference system fixed in the center of gravity, an energy of the order of $\Delta E_n = m/m_D^2 \cdot \Delta p^2/2$. If $\Delta p \simeq 2p$, then $\Delta E_n \simeq 2E$. For E = 15 Mev, $\Delta E \simeq 30$ Mev, which considerably exceeds the binding energy of the deuteron (2.19 Mev). This means that in diffraction at large angles the deuteron can dissociate ("diffraction breakup"), or, in any case, be deformed. In other words, these considerations do not permit us to assume a priori that the scattering of deuterons at sufficiently large angles can be regarded as the diffraction of a wave corresponding to the motion of the deuteron as a whole. Therefore, the experimental data which indicate the validity of the optical model for the scattering of deuterons at large angles contain very vital information: they show that the effects of deformation of the deuteron during the scattering process are unimportant.

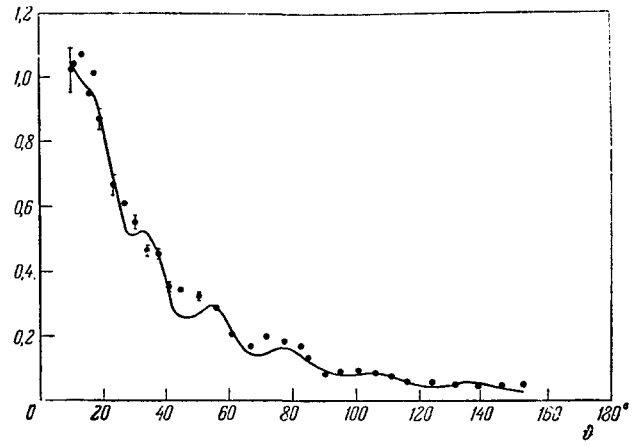

FIG. 25. $d\sigma_s/d\Omega$ for 15-Mev deuterons. The scatterer was Rh. The solid curve gives computations on the optical model with volume absorption (ϑ in the c. m. system).

The first papers on the optical model for deuterons date from approximately 1956.[20] At present, the study of the optical model for deuterons is still in its initial stages. It is not clear in particular (because of the lack of detailed experimental data) to what extent the optical model correctly describes the behavior of the deuteron cross sections σ_s and σ_r as a function of energy and mass number. No test has been made of

Table II. Parameters of the optical potential for deuterons

Deuteron energy (Mev)	Element	V_0 (Mev)	W_0 (Mev)	r_0 (fermi)	a (fermi)
13.5	Ni	59	19	1.43	0.63
	Sn	60	10.5	1.60	0.62
	Au	50	9	1.50	0.66
15	Al	55	25	1.50	0.60
	Ti	59	21	1.50	0.60
	Rh	52	12	1.62	0.60
	Sn	55	11	1.60	0.58
	Pd	53	11	1.62	0.58
	Ta	48.5	9	1.55	0.53
	Au	50	9	1.55	0.66
	Pb	48.5	9	1.52	0.63

the model with surface absorption, which for deuterons may be especially important because of peripheral processes of the type of the stripping reaction. The introduction of surface absorption should lead in particular to a smoothing out of the variation of parameters of the optical potential as a function of A.

Finally, it should be clarified just how well the optical model for deuteron scattering describes polarization phenomena. Since the spin of the deuteron is 1, polarization phenomena can differ significantly from those which occur in the case of nucleons. Let us consider this problem in a little more detail. The projection of the deuteron spin on any direction can take on three values, +1, 0, and −1. Let us agree to denote the states with projection +1, 0, and −1 by subscripts 1, 2, and 3 respectively. The scattering amplitude is a three-by-three matrix

$$f=\begin{Bmatrix} f_{11} & f_{12} & f_{13} \\ f_{21} & f_{22} & f_{23} \\ f_{31} & f_{32} & f_{33} \end{Bmatrix}, \tag{81}$$

$$\frac{d\sigma_s}{d\Omega}=\sum_{\alpha\beta}|f_{\alpha\beta}|^2 \qquad (\alpha, \beta=1, 2, 3), \tag{82}$$

$$\frac{d\sigma_{\alpha\beta}}{d\Omega}=|f_{\alpha\beta}|^2, \tag{83}$$

where $d\sigma_{\alpha\beta}$ is the scattering cross section corresponding to a process in which the deuteron was in spin state α before the scattering and goes into spin state β after the scattering. Let us see what are the characteristics of the spin alignment of the scattered deuteron beam. In the case of nucleons, the only characteristic was the polarization, the ratio of the difference in cross sections for the two possible spin projections in the final state to the sum of these cross sections. This definition can be formulated in the following way, which is more convenient for generalization: the polarization is the ratio of the average value of the spin projection on a given direction to the spin of the particle. In fact, in the case of spin $\frac{1}{2}$ (nucleon) we had, according to formula (44),

$$P_\nu=\frac{d\sigma_+-d\sigma_-}{d\sigma_s}\equiv\frac{1}{2}\left\{\left(+\frac{1}{2}\right)\frac{d\sigma_+}{d\sigma_-}+\left(-\frac{1}{2}\right)\frac{d\sigma_-}{d\sigma_s}\right\}=\frac{\bar{s}_\nu}{s}, \tag{83a}$$

where $\bar{s}_\nu$ is the average value of the spin projection and s is the spin of the nucleon.

Generalizing this definition for spin 1 (the deuteron), we have

$$P_\nu=\frac{\bar{s}_\nu}{s}=(+1)\frac{d\sigma_+}{d\sigma_s}+0\,\frac{d\sigma_0}{d\sigma_s}+(-1)\frac{d\sigma_-}{d\sigma_s}\equiv\frac{d\sigma_+-d\sigma_-}{d\sigma_s}, \tag{83b}$$

where

$$d\sigma_+=\sum_\alpha|f_{\alpha1}|^2, \quad d\sigma_-=\sum_\alpha|f_{\alpha3}|^2, \quad d\sigma_0=\sum_\alpha|f_{\alpha2}|^2. \tag{84}$$

In the case of deuterons, P_ν is, however, not the only characteristic of the alignment of the scattered beam, since $d\sigma_0$ does not even appear in P_ν. In fact, we may say that the spins of the particles of the beam are oriented at random if

$$d\sigma_+=d\sigma_-=d\sigma_0. \tag{85}$$

If $P_\nu = 0$, it then follows only that

$$d\sigma_+=d\sigma_-,$$

but not equation (85). Thus, if $P_\nu = 0$, but $d\sigma_+ = d\sigma_- \neq d\sigma_0$, the beam is ordered to some extent since the numbers of particles with different spin projections are not equal to one another. Let us therefore introduce still another characteristic of the alignment of the beam, which we shall call the quadrupolarization Q_ν:

$$Q_\nu=\frac{d\sigma_++d\sigma_--2d\sigma_0}{3d\sigma_s}. \tag{86}$$

If the beam is completely disordered, i.e., if we have Eq. (85), then $Q_\nu = P_\nu = 0$. Conversely, if $Q_\nu = P_\nu = 0$, then (85) is satisfied, i.e., the beam is completely disordered. But if either one of the quantities (Q_ν or P_ν) is different from zero, then the orientation of the spins of the particles in the beam is no longer random. The quadrupolarization Q_ν can also be expressed in terms of the average value $\overline{S_\nu^2}$ of the square of the spin projection of the deuteron:

$$\overline{S_\nu^2}=\frac{d\sigma_++d\sigma_-}{d\sigma_s}. \tag{87}$$

Noting that

$$\frac{d\sigma_0}{d\sigma_s}=1-\overline{S_\nu^2}, \tag{88}$$

we find

$$Q_\nu=\frac{3\overline{S_\nu^2}-2}{3}. \tag{89}$$

Let us now see what experimentally observable phenomena in deuteron scattering occur because of the presence of the two polarization characteristics P_ν and Q_ν. For this purpose we note that the matrix of the scattering amplitudes f, just as in the case of nucleons, can be represented as a linear combination of certain basis matrices. The number of such basis matrices should be equal to the number of matrix elements f, i.e., nine. These basis matrices are the following:

$$1=\begin{pmatrix}1&0&0\\0&1&0\\0&0&0\end{pmatrix}, \quad I_1=\frac{i}{\sqrt{2}}\begin{pmatrix}0&1&0\\1&0&1\\0&1&0\end{pmatrix},$$
$$I_2=\frac{i}{\sqrt{2}}\begin{pmatrix}0&1&0\\-1&0&0\\0&-1&0\end{pmatrix}, \quad I_3=\begin{pmatrix}1&0&0\\0&0&0\\0&0&-1\end{pmatrix}, \tag{90}$$

$$Q^{ij}=I_iI_j+I_jI_i-\frac{4}{3}\delta_{ij} \qquad (i, j=1, 2, 3). \tag{91}$$

The independent matrices Q^{ij} are five in number, since, first of all

$$Q^{ij}=Q^{ji} \tag{92}$$

and secondly

$$\sum_i Q^{ii} = 0, \tag{93}$$

i.e.,

$$Q^{33} = -Q^{11} - Q^{22}. \tag{93a}$$

The matrices I_i play the same role in the theory of particles with spin 1 as the Pauli matrices $\sigma^{(i)}$ played in the theory of spin-$\frac{1}{2}$ particles. The equations (90) and (91) thus determine nine independent matrices of third order, in terms of which one can expand the matrix f:

$$f = \frac{a}{\sqrt{3}} \cdot 1 + \sum_i \frac{b'}{\sqrt{2}} I_i + \frac{\sqrt{3}}{8} \sum_{i,j} c_{ij} Q^{ij}. \tag{94}$$

According to (82), the differential scattering cross section $d\sigma_S$ is

$$d\sigma_s = \sum_{\alpha,\beta} f_{\alpha\beta} f^*_{\alpha\beta} \equiv \sum f^*_{\alpha\beta} f_{\alpha\beta} = \sum_\beta (f^* f)_\beta = \mathrm{Sp}\, f^+ f, \tag{95}$$

where f^+ is the Hermitian conjugate of the matrix f:

$$f^+_{\alpha\beta} = f^*_{\beta\alpha}. \tag{96}$$

Since the matrices I_i and Q^{ij} are Hermitian, i.e.,

$$I_i^+ = I_i, \quad Q^{ij+} = Q^{ij}, \tag{96a}$$

and since, in addition,

$$\mathrm{Sp}\, I_i = \mathrm{Sp}\, Q^{ij} = \mathrm{Sp}\, I_k Q^{ij} = 0, \tag{97}$$

$$\mathrm{Sp}\, I_i I_j = 2\delta_{ij}, \tag{98}$$

$$\mathrm{Sp}\left\{ \sum_{ij,\,kl} c_{ij} c^*_{kl} Q^{ij} Q^{kl} \right\} = \frac{8}{3} \sum_{ij} |c_{ij}|^2, \tag{99}$$

then, substituting (94) in (95) and using (96) — (99), we find

$$d\sigma_s = |a|^2 + \sum_i (b'_i)^2 + \sum_{ij} (c_{ij})^2. \tag{100}$$

Now arguing in exactly the same way as in Sec. 1, we arrive at the conclusion that the quantities b'_i are the components of a vector directed along **n**:

$$\mathbf{b}' = b'\mathbf{n}, \tag{101}$$

and that the five independent quantities c_{ij} form a symmetric tensor of rank two. Using the three orthogonal unit vectors **m**, **l**, and **n** which are at our disposal, we may represent c_{ij} in the form

$$c_{ij} = (c_m m_{ij} + c_l l_{ij} + c_n n_{ij})\sqrt{8}, \tag{102}$$

where

$$m_{ij} = m_i m_j \tag{103}$$

(l_{ij} and n_{ij} are determined by similar equations) and c_l, c_m, and c_n are scalars depending on the scattering angle ϑ. The fact that tensors of the type $n_i m_j$, $n_i l_j$ do not appear in c_{ij} is related to the invariance of $d\sigma_{\alpha\beta}$ with respect to space inversion. Tensors of the type $l_i m_j$ do not appear because of the invariance of $d\sigma_S$ with respect to time reversal (then $\mathbf{m} \to \mathbf{m}$, $\mathbf{l} \to -\mathbf{l}$).

Thus we finally have:

$$f = \frac{a}{\sqrt{3}} 1 + \frac{b'}{\sqrt{2}} \mathbf{nl} + \sqrt{\frac{3}{8}} \sum c_{ij} Q^{ij}, \tag{104}$$

where c_{ij} is given by (102).

We now express the quantities P_ν and Q_ν in terms of a, b′ and c_{ij}. To do this we first note that formula (53) for the polarization of the nucleons in a direction ν making an angle ϑ with the vector, can be rewritten in the form*

$$P_\nu = \frac{ab'^* + a^* b'}{|a|^2 + |b'|^2} \mathbf{n\nu} \equiv \frac{\mathrm{Sp}\, f^* f \sigma \nu}{\mathrm{Sp}\, f^+ f}. \tag{104a}$$

Similarly, the polarization of the deuteron beam after the scattering is given by the formula

$$P_\nu = \frac{\mathrm{Sp}\, f^+ f \mathbf{l}\nu}{\mathrm{Sp}\, f^+ f} = \frac{ab'^* + a^* b'}{|a|^2 + |b'|^2 + \sum_{ij} |c_{ij}|^2} \mathbf{n}\nu. \tag{105}$$

The quadrupolarization Q_ν along the direction ν is given by the expression

$$Q_\nu = \frac{\mathrm{Sp}\, f^+ f Q^{ij} \nu_{ij}}{\mathrm{Sp}\, f^+ f} = \frac{1}{\sqrt{8}} \frac{ac^*_{ij} + a c^*_{ij}}{|a|^2 + |b'|^2 + \sum_{ij} |c_{ij}|^2} \nu_i \nu_j. \tag{106}$$

Using formula (102) for the c_{ij} and noting that

$$\sum_{ij} m_{ij} \nu_{ij} = (\mathbf{m}\nu)^2, \tag{107}$$

we get

$$Q_\nu = Q^\nu_m + Q^\nu_l + Q^\nu_n, \tag{108}$$

where

$$Q^\nu_m = \frac{ac^*_m + a^* c_m}{|a|^2 + |b'|^2 + \sum_{ij} |c_{ij}|^2} (\mathbf{m}\nu)^2. \tag{109}$$

Similar equations give Q^ν_l and Q^ν_n. The quantities Q^ν_m, Q^ν_l, and Q^ν_n are the components of the quadrupolarization Q_ν in the directions **m**, **l**, and **n**. From formulas (105), (108), and (109) we see that the polarization is determined by the quantity b′, and the quadrupolarization by the quantities c_m, c_l, and c_n. From formulas (105), (108), and (109) we see also that $P_\nu = 0$ if $\nu \perp \mathbf{n}$. However, the quadrupolarization Q_ν will in general be different from zero. If $Q_\nu \neq 0$, then we say that the beam is "aligned" along the direction ν. If $P_\nu \neq 0$, then we say that the beam is polarized along the direction ν. Since Q_ν depends quadratically on the vector ν, then $Q_\nu = Q_{-\nu}$. This means that all effects related to beam alignment along some direction ν are not changed when we replace ν by $-\nu$. Therefore the possible anisotropy in angular distributions in scattering of a beam of aligned particles should exhibit symmetry with respect to the plane perpendicular to ν.

Let us now consider the question of how one can measure P_ν and Q_ν, occurring as a result of the

*ν is the direction of the "axis of quantization" i.e., the direction along which we take the spin projection; for our choice of the matrices σ and **l** this direction is the z axis.

scattering of completely unpolarized deuterons by some nucleus. We know that the polarization P_y can be measured by performing a second scattering and observing the dependence of the intensity of the second-scattered particles on the angle between the planes of the first and second scatterings, i.e., on $\mathbf{n}\cdot\mathbf{n}'$, where

$$\mathbf{n}' = \frac{[\mathbf{k}'\mathbf{k}'']}{2k \sin \vartheta'/2}. \tag{110}$$

Here $\mathbf{k}''$ is the wave vector of the twice-scattered particles, ϑ is the angle between $\mathbf{k}'$ and $\mathbf{k}''$ (the angle of the second scattering).

The intensity dJ of the second scattered particles will obviously be equal to the following expression:

$$dJ = \frac{J_0\, d\sigma_s\, d\sigma_s'}{L^2\, d\Omega} F, \tag{111}$$

$$F = \frac{\{\sum_{\alpha\beta\gamma} |f_{\alpha\beta}|^2 |f_{\beta\gamma}|^2\}}{\{\sum_{\alpha\beta} |f_{\alpha\beta}|^2\}\{\sum_{\alpha\beta} |f'_{\alpha\beta}|^2\}}, \tag{112}$$

where J_0 is the current density in the initial beam, L is the distance between the first and second scatterers, and the primed quantities refer to the second scattering. The sum F can be calculated without any special technical tricks only in the simple case of spin $\frac{1}{2}$. For larger spin values, and in particular already for spin 1, such a "head-on" calculation becomes too complicated. The artifice used in these cases is the following. We may note that the quantities

$$\varrho_{\alpha\beta} = \frac{\sum_\gamma f^*_{\alpha\gamma} f_{\gamma\beta}}{d\sigma_s} \tag{112a}$$

form a Hermitian matrix $\rho = f^+ f$. This matrix is called the density matrix. The density matrix, according to its definition, can depend only on observable quantities, so that its expansion in terms of the matrices I_i and Q_i must have the form

$$\varrho = \frac{1}{3} + \frac{1}{\sqrt{2}} P \mathbf{n} \mathbf{I} + \frac{3}{8} \sum_{ij} (Q_m m_{ij} + Q_l l_{ij} + Q_n n_{ij}) Q^{ij}, \tag{113}$$

where

$$P = P_n, \tag{114}$$

$$Q_m = Q_m^{(m)}, \quad Q_l = Q_l^{(l)}, \quad Q_n = Q_n^{(n)}. \tag{115}$$

The quantities Q_m, Q_l, and Q_n are the quadrupolarizations along the physically distinguished directions $\mathbf{m}$, $\mathbf{l}$, and $\mathbf{n}$.

The density matrix ρ' of the second scattering, which we shall call the density matrix of the analyzer, has a form which is entirely analogous to (113), with the one difference that the quantities P' and Q' which appear in it refer to the second scattering. The quantity F which we are interested in then has the form

$$F = \sum_\alpha \varrho_{\alpha\alpha} \varrho'_{\alpha\alpha}. \tag{116}$$

We now note that F should be invariant with respect to rotations of the coordinate system. The matrices ρ and ρ' will then transform according to the law

$$\varrho \to D\varrho D^{-1}, \qquad \varrho' \to D\varrho' D^{-1}, \tag{117}$$

where D is a matrix depending on the parameters of the rotation. But this means that we may always turn the coordinate system so that one of the matrices, for example, the matrix ρ', becomes diagonal (since any Hermitian matrix can always be brought to diagonal form):

$$\varrho'_{\beta\alpha} = \delta_{\beta\alpha} \varepsilon_\alpha. \tag{117a}$$

Then (116) can be written as follows:

$$F = \sum \varepsilon_\alpha \varrho_{\alpha\alpha} \equiv \sum_{\alpha,\beta} \varrho_{\alpha\beta} \delta_{\beta\alpha} \varepsilon_\alpha = \mathrm{Sp}\, \varrho\varrho'. \tag{118}$$

As already noted, F is invariant with respect to rotation, and Sp also does not change under the transformations (117);* therefore (118) will be valid in any coordinate system, independently of whether either of the matrices ρ, ρ' is diagonal or not.

Substituting the formulas (113) for ρ and ρ' in (118) and using relations (97) — (99), we find:

$$F = \frac{1}{3} + \frac{1}{2} PP' \mathbf{nn}' + \frac{3}{8} (Q_m Q'_{m'} (\mathbf{mm}')^2 + Q_l Q'_{l'} (\mathbf{ll}')^2 + Q_n Q'_{n'} (\mathbf{nn}')^2. \tag{119}$$

Formula (122) contains the complete angular correlation of the double-scattered deuterons. It is interesting to compare it with the analogous expression for the double scattering of nucleons:

$$F_{\mathrm{nucl}} = \frac{1}{2}(1 + PP' \mathbf{nn}'). \tag{120}$$

Formula (120) shows that, because of the presence of quadrupolarization, the azimuthal asymmetry after the second scattering will have the form

$$\alpha + \beta \cos\varphi + \gamma \cos^2\varphi, \tag{121}$$

where φ is the angle between $\mathbf{n}$ and $\mathbf{n}'$, and the measurement of the coefficient of $\cos^2\varphi$ enables us to determine the quadrupolarization Q_n, if we know the quadrupolarization Q'_n of the analyzer. We note that in the case of nucleons there is no term quadratic in $\cos\varphi$, as we see from formula (120).

The study of polarization phenomena in deuteron scattering is of great interest, since it enables us to investigate how completely the optical model describes the scattering process and, consequently, to what extent it reflects reality if we are dealing with composite particles. From the consideration of the general form of the scattering amplitude carried out above, it is clear that the optical potential can have a more complicated structure in the case of the deuteron. Namely, instead of the usual central potential and spin-orbit interaction, for describing the quadrupolarization it may be convenient to introduce additional terms of the type

*) $\mathrm{Sp}\, \varrho\varrho' \to \mathrm{Sp}\, D\varrho\varrho' D^{-1} = \sum_{\alpha,\beta,\gamma,\delta} D_{\alpha\beta}\varrho_{\beta\gamma}\varrho'_{\gamma\delta} D^{-1}_{\delta\alpha} = \sum D^{-1}_{\delta\alpha} D_{\alpha\beta}\varrho_{\beta\gamma}\varrho'_{\gamma\delta}$
$= \sum \delta_{\delta\beta}\varrho_{\beta\gamma}\varrho_{\gamma\delta} = \sum_{\gamma,\beta} \varrho_{\beta\gamma}\varrho'_{\gamma\beta} = \mathrm{Sp}\, \varrho\varrho'.$

$$U_Q = \sum_{ij} (V_Q(r) r_i r_j + V'_Q(r) \nabla_i \nabla_j + V''_Q(r) \hat{l}_i \hat{l}_j) Q^{ij}. \quad (122)$$

A potential of the type (122) for deuterons has as yet not been studied theoretically because of the practically complete absence of experimental data concerning polarization phenomena in deuteron scattering. In all probability, $U_Q(\mathbf{r})$ should be treated as a surface potential, and one should begin its investigation with a term containing the angular momentum operator $\hat{l}_i$. It is just this term which is important for azimuthal asymmetry in double scattering, i.e., for experiments which may possibly be carried out first, since they are entirely analogous to the existing experiments with protons.

5. Scattering of Heavy Ions

Satisfactory experimental data on angular distributions of heavy ions elastically scattered from nucleons (such as, N^{14}, O^{16}, etc.) have appeared only very recently. In particular, this applies to scattering at large angles. Therefore the experimental data available at present are very few in number. Nevertheless, it follows clearly from these data that the black nucleus model is not applicable to scattering of heavy ions. An extremely convincing illustration is given in Fig. 27, in which we reproduce the results of a recently published paper by Reynolds, Goldberg, and Kerlee[21] on the scattering of O^{16} ions of energy 164 Mev by Au^{197}. The abscissa is the scattering angle in the center-of-mass system, and the ordinate the ratio $d\sigma_S/d\sigma_R$. The data for large scattering angles show only the upper limit for the intensity of the scattered particles. The solid curve in this figure is calculated by the black nucleus model considered in Sec. 3, with $l' = 89$. As we see from the figure, at angles greater than 40° the experimental data and the theoretical computations on the black nucleus model are in marked disagreement. The situation is not rectified if one includes waves which tunnel through the centrifugal barrier (dashed curve).

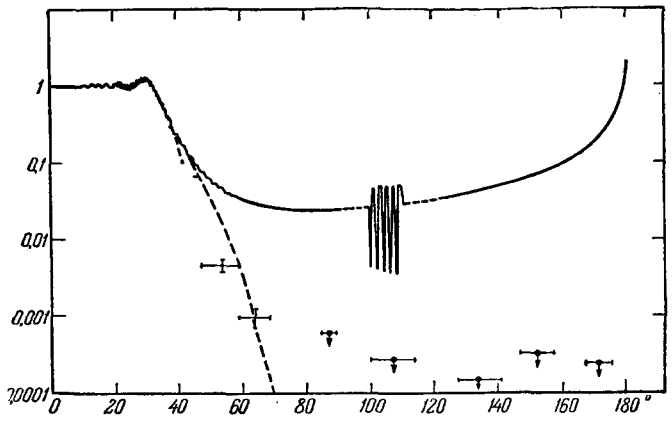

FIG. 27. $d\sigma_S/d\sigma_R$ for 165-Mev O^{16} ions. The scatterer is Au. The solid curve is computed on a black body model ($l' = 89$).

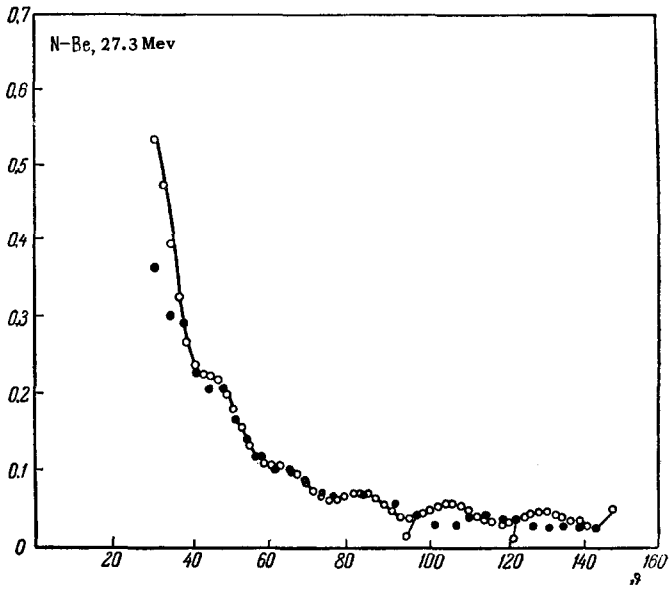

FIG. 28. $d\sigma_S/d\sigma_R$ for N^{14} ions with an energy of 27.3 Mev. The scatterer is Be. The black circles are experimental data; the white circles, theoretical computation for the optical model with surface absorption and diffuse edge. The parameters were: V_0 = 50 Mev, W_0 = 16 Mev, r_0 = 1.23 fermi, a = 0.65 fermi, b = 1.125 fermi.

On the other hand, the agreement of the experimental data with the results of computations on the optical model should be regarded as extremely satisfactory. This is indicated, for example, by the data of Bassel and Drisko,[22] which is shown in Figs. 28 — 29. These results are for the scattering of N^{14} ions, with an energy of 27.3 Mev, by carbon and beryllium nuclei. The theoretical results shown in Figs. 28 and 29 were obtained from a model with surface absorption. Satisfactory agreement of theory and experiment for this case is also obtained using volume absorption, with

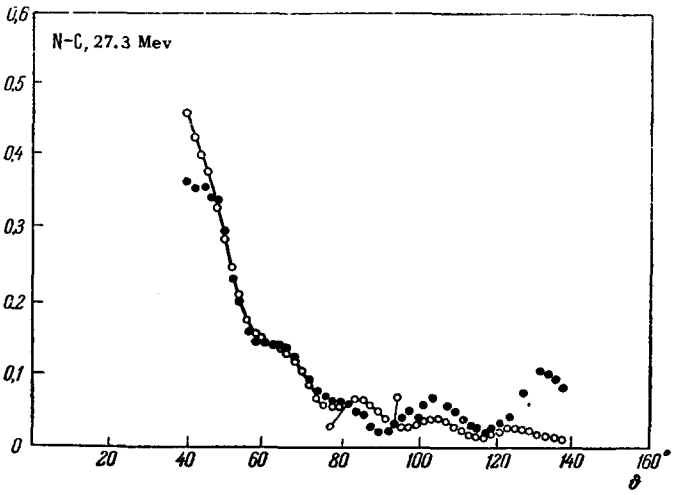

FIG. 29. $d\sigma_S/d\sigma_R$ for N^{14} ions with an energy of 27.3 Mev. The scatterer is C. The notation is the same as in Fig. 28. The parameters were: V_0 = 47 Mev, W_0 = 9 Mev, r_0 = 1.275 fermi, a = 0.645 fermi, b = 1.25 fermi.

the following values of the parameters of the optical potential (the Woods-Saxon potential was used):

$$V_0 = 48 \text{ Mev}, \quad W_0 = 5.75 \text{ Mev},$$
$$r_0 = 1.275 \cdot 10^{-13} \text{ cm}, \quad a = 0.575 \cdot 10^{-13} \text{ cm}.$$

The mean free path Λ_N for the N^{14} nucleus in nuclear material, as calculated with these data, is $\Lambda_N \simeq 2 \times 10^{-13}$ cm. This is much greater than the mean free path which one would expect if one started from the cross section for collision of N^{14} with a free nucleon. Just as in the case of deuterons, investigations on the optical model for heavy ions are at present in an early stage of development. In particular, there are no sufficiently detailed data on total cross sections, and no polarization experiments have been carried out. Of course, only after a comparison of such data with the results of computations on the optical models can one state to what extent the optical model is close to reality in describing the interaction of composite particles with nuclei. However, one important conclusion can probably already be drawn. This is the statement that nuclear matter is much more transparent than was previously assumed, not only for nucleons, but also for composite particles.

6. The Optical Model and Direct Processes

As we know, as a result of investigations in recent years it has become clear that the Bohr picture of the mechanism of nuclear reactions, as processes which proceed via an intermediate state of formation and decay of a compound nucleus, is not in agreement with experiment in many cases. This manifests itself in:

a) a difference between the energy spectrum of emerging particles from that for a Maxwellian evaporation spectrum;

b) the asymmetry of angular distributions around $\vartheta = 90°$, where ϑ is the angle (in the center-of-mass system) between the momenta of the incident particles and the reaction products;

c) anomalously large yields of composite particles (α-particles, deuterons) compared with the yield of nucleons, when the emergence of the latter is not forbidden by any known selection rules (for example, the reaction $N^{14}(n, \alpha)B^{11}$ is 30 times more probable than $N^{14}(n, p)C^{14}$, for the same neutron energies, 1.8 — 4.2 Mev).

In the light of these facts, it is extremely interesting to attempt to treat the so-called direct nuclear processes as reactions in which the impinging nucleon ejects the composite particle (deuteron, α particle, etc.) from the nucleus, where such a particle is already prepared and existing in the nucleus. Such an approach to the theory of direct processes, which has been discussed earlier, is especially interesting at present since, as we have explained in the preceding paragraphs, the mean free paths of composite particles in nuclear matter are large. This means that a composite particle, formed in the nucleus at a certain time, will exist in it for a relatively long time, on the average over a period of the order of $\tau \approx \Lambda/v$ where v is the velocity of the particle in the nucleus.

Since, as is now clear, Λ is of the same order of magnitude as the nuclear radius R, then, first of all, the probability that the composite particle which appears in the nucleus will not be broken up during the time $\Delta t \simeq R/v'$ after the passage through the nucleus of the impinging particle (with velocity v'), is comparable to unity, and, secondly, because of the transparency of nuclear matter, such a composite, intranuclear particle will have a considerable probability for emerging from the nucleus.

Since as a result of theoretical and experimental studies of the optical model, we at least know the orders of magnitude of the parameters of the optical model for a composite particle, there arises an entirely definite problem of developing a theory of processes of "direct ejection" which should quantitatively relate the cross sections of these processes with the data of the optical model. Thus one will establish the internal connection between the results of two different groups of nuclear experiments, experiments on the scattering of particles by nuclei and experimental data on direct nuclear interactions. If it turns out that these two groups of experimental facts can actually be brought into quantitative agreement with one another (in some conventional sense; for more detail concerning this, see reference 23), then this will be a strong argument in favor of the possibility of the existence in the nucleus over a reasonably long time of complex associations of the type of α particles, deuterons, and other particles. The establishment of such a fact would undoubtedly be one of the most important results in the evolution of our picture of the structure of atomic nuclei and of the dynamics of nuclear processes.

[1] Feshbach, Porter, and Weisskopf, Phys. Rev. **90**, 166 (1953).

[2] Feshbach, Porter, and Weisskopf, Phys. Rev. **96**, 448 (1954).

[3] H. H. Barschall, Phys. Rev. **86**, 431 (1952); M. Walt and H. H. Barschall, Phys. Rev. **93**, 1062 (1954).

[4] R. D. Woods and D. S. Saxon, Phys. Rev. **95**, 577 (1954).

[5] P. É. Nemirovskii, DAN SSSR **101**, 257 (1955).

[6] Luk'yanov, Orlov, and Turovtsev, Nuclear Phys. **8**, 325 (1958).

[7] I. McCarthy, Proceedings of the International Conference on the Nuclear Optical Model, Florida, 1959, p. 24.

[8] F. E. Bjorklund and S. Fernbach, Phys. Rev. **109**, 1295 (1958).

[9] R. E. Peierls, Proceedings of the International Conference on the Nuclear Optical Model, Florida 1959, p. 262.

[10] H. H. Barschall, International Conference on Nuclear Physics, Paris, 1958, p. 7; Crosby Lockwood, London, 1959.

[11] P. É. Nemirovskii, Sovremennye Modeli Atomnogo Yadra (Contemporary Models of the Atomic Nucleus), Moscow, Atomizdat, 1960.

[12] I. I. Levintov, DAN SSSR **101**, 249 (1955); **107**, 240 (1956), Soviet Phys. Doklady **1**, 175 (1957).

[13] L. Rosen, Proceedings of the International Conference on the Nuclear Optical Model, Florida, 1959, p. 185.

[14] L. Rosen, Proceedings of the International Conference on the Nuclear Optical Model, Florida, 1959, p. 72.

[15] J. S. Blair, Phys. Rev. **95**, 1218 (1954).

[16] J. S. Blair, Phys. Rev. **108**, 827 (1957).

[17] G. Igo and R. M. Thaler, Phys. Rev. **106**, 126 (1957).

[18] W. B. Cheston and A. E. Glassgold, Phys. Rev. **106**, 1215 (1957).

[19] M. A. Melkanoff, Proceedings of the International Conference on the Nuclear Optical Model, Florida, 1959, p. 207.

[20] I. S. Shapiro and E. I. Dolinskii, Physica **22**, 1164 (1956).

[21] Reynolds, Goldberg, and Kerlee, Phys. Rev. **119**, 2009 (1960).

[22] R. H. Bassel and R. M. Drisko, Proceedings of the International Conference on Nuclear Structure, Kingston, Canada, 1960, p. 212.

[23] I. S. Shapiro, JETP **41**, 1616 (1961), Soviet Phys. JETP **14**, in press.

Translated by M. Hamermesh